TECHNICAL UNIVERSITY OF LIBEREC
Faculty of Mechatronics, Informatics
and Interdisciplinary Studies

Adaptive assistance considering human factors for industrial carts

Dissertation

Study programme: P2612 – Electrical engineering and informatics
Study branch: 2612V045 – Technical cybernetics

Author: **Ing. Dmitry Kochubey**
Supervisor: doc. Ing. Petr Tůma, CSc.

Liberec 2020

TECHNICKÁ UNIVERZITA V LIBERCI
Fakulta mechatroniky, informatiky
a mezioborových studií

Elektrická pomoc pro průmyslové vozíky

Disertační práce

Studijní program: P2612 – Elektrotechnika a informatika
Studijní obor: 2612V045 – Technická kybernetika

Autor práce: **Ing. Dmitry Kochubey**
Vedoucí práce: doc. Ing. Petr Tůma, CSc.

Liberec 2020

Declaration

I hereby certify that I have been informed that Act 121/2000, the Copyright Act of the Czech Republic, namely Section 60, School-work, applies to my dissertation in full scope. I acknowledge that the Technical University of Liberec (TUL) does not infringe my copyrights by using my dissertation for TUL's internal purposes.

I am aware of my obligation to inform TUL on having used or licensed to use my dissertation in which event TUL may require compensation of costs incurred in creating the work at up to their actual amount.

I have written my dissertation myself using literature listed therein and consulting it with my supervisor and my tutor.

I hereby also declare that the hard copy of my dissertation is identical with its electronic form as saved at the IS STAG portal.

Date:

Signature:

Abstrakt

Tato výzkumná práce se zaměřuje na probádání fyzikální interakce, která vzniká mezi lidským operátorem a průmyslovým vozíkem s pohonem (IPAC). Cílem výzkumu je zlepšit spolupráci člověka a IPAC tím, že se nalezne správný mechanický design a způsob inteligentní kontroly za účelem dosažení takového stavu, ve kterém vozík umí rozpoznat záměr operátora a je schopen nastavit svoje parametry tak, aby došlo k lepší interakci vozíku s člověkem a bylo zajištěno pohodlí a celkový výkon.

V rámci této disertační práce byl vyvinut prototyp průmyslového vozíku, který byl vybaven sadou senzorů na měření parametrů interakce člověka s vozíkem. Tento vyvinutý průmyslový vozík je schopen rozpoznat záměr člověka na základě sledování parametrů procesu interakce. Na začátku této práce byla provedena analýza současného stavu techniky a byly vybrány nejslibnější kontrolní techniky. Analyzovali jsme součásti průmyslového vozíku a vytvořili jsme kinematický a dynamický popis modelu. Tento vyvinutý vozík má dva stupně volnosti a byly použity regulátory impedance tak, aby ovládaly oba stupně.

Přesto je však tato disertační práce hlavně zaměřena na zpětnou vazbu a pohodlí člověka. Proto byl proveden soubor experimentů s cílem odhadnout účinky parametrů proměnné impedance, co se týče regulátoru translačních a rotačních pohybů. Za účelem vyhodnocení emocionální zpětné vazby lidského operátora byl vyvinut objektivní párový dotazník. Ve výsledku jsme našli vztah mezi nezávislými proměnnými, jako jsou například parametry komfortu obsluhy. Pomocí regresivní analýzy jsme zjistili, že ne všechny parametry regulátoru impedance mají významný vliv na interakci. Také jsme zjistili, že parametry impedance pro pohodlnou interakci se liší u různých operátorů. Zjistili jsme, že existuje významná korelace mezi průměrnou a standardní odchylkou absolutní hodnoty interakční síly a rychlostí vozíku a pohodlím člověka.

Pomocí výsledků regresivní analýzy jsme použili algoritmus zesíleného učení, který mohl přepínat stavy regulátorů impedance podle záměrů operátora. V rámci této diplomové práce je představen proces vývoje vozíku a metodologie výzkumu.

Abstract

The research work is focused on the study of physical interaction between the human-operator and an industrial power-assisted cart (IPAC). The research goal is to improve the cooperation between human and IPAC by finding a proper mechanical design and methods of intelligent control in order to achieve a state in which the cart can recognize operator's intention and adjust its parameters for a better human-cart interaction, comfort and overall performance.

In the scope of the thesis a prototype of an industrial cart was developed and equipped with a set of sensors to measure the human-cart interaction parameters. Developed industrial cart could recognize human intention by observing interaction process parameters. In the beginning of the work the analysis of the state of art was performed and the most promising control techniques were selected. We analyzed the components of the industrial cart and created the kinematic and dynamic description of the model. The developed cart has two degrees of freedom and impedance controllers were implemented to manage both of these degrees.

Nevertheless, The thesis is mainly focused on human feedback and comfort. Therefore, a set of experiments was performed to estimate the effect of variable impedance parameters for the controller of transnational and rotational motions. In order to evaluate emotional feedback of the human-operator an objective pair-based questionnaire was developed. As a result, we found a relationship between independent variables such as impedance control parameters and operator's comfort experience. Using regression analysis we found out that not all the parameters of the impedance controller have a significant effect on the interaction. We also learned that the impedance parameters for comfortable interaction are different for different operators. We learned that there is a strong correlation between the mean and the standard deviation of absolute value of interaction force and cart speed and human comfort.

Using the regression analysis results we implemented the reinforcement learning algorithm that could switch states of the impedance controllers according to the operator's intention. The process of cart development and the research methodology is presented in the scope of the thesis.

Acknowledgements

I would like to express my gratitude to everyone who helped me in my studies leading to this dissertation. First and foremost, I offer my sincerest gratitude to my supervisor, doc. Ing. Petr Tůma, CSc. (Department of Mechatronics and Technical Informatics (MTI)), who provided his supervision and valuable guidance through my research experience. I also thank doc. Dr. Mgr. Ing. Jaroslav Hlava (MTI) for his time and consultations in the field of adaptive control algorithms and simulation.

Additionally, I would like to extend my special thanks to doc. RNDr. Jaroslav Mlýnek, CSc., prof. Ing. Aleš Richter, CSc. and Mgr. Václav Bittner for their support and advice related to human-oriented research and mathematical modeling. I appreciate support of Ing. Pavel Jandura, Ph.D. for his support in electrical wiring of the first platform prototype.

I have special acknowledgments to doc. Ing. Michal Petrů, Ph.D., Ing. Voženílek Robert, Ph.D. and Josef Stuchlik for their support in mechanical construction of the platform and data analysis. Further, I highly appreciate the effort of Professor Kouhei Ohnishi (Keio University, Japan), who has shared his extraordinary experience in the field of human-robot interaction and soft robotics.

I am deeply grateful to Dr. Fillia Makedon (Department of Computer Science and Engineering University of Texas at Arlighton (UTA)) and her colleagues for the conference experience and cooperation. Moreover, I have greatly progressed in many areas thanks to my internship at Linz Center of Mechatronics (LCM GmbH). Close collaborations and discussions with the smart and cordial group of colleagues helped me to reach the level that would have been impossible to achieve on my own. There are too many to name all of them, but I would like to mention MSc. Kalus Pendl who was always incredibly helpful and supportive.

I would like to thank Phd. David Krcmarick as my office mate he was the first person to bounce my ideas off and to share the joy and sorrows of my research life. Last but not least, I would like to take the opportunity to express my gratitude to the Siemens colleagues in the name of MSc. Johannes Hofmann and Dr. Michael Fielder for their understanding and support. In the end I would like to express my deep gratitude and special thanks to whole my family for their support, patience and love throughout the years.

Contents

List of Figures

List of Tables

List of abbreviations

TUL	Technická univerzita v Liberci
FM	Fakulta mechatroniky, informatiky a mezioborových studií Technické univerzity v Liberci
IPAC	Industrial power assisted cart
pHRI	Physical human – robot interaction
MAFs	Maximum acceptable interaction forces
MSD	Mass-Spring-Damper
RPE	Rate Per Excretion
SWI	Size-Weight Illusion
RL	Reinforcement Learning
MDP	Markov Decision Process
TD	Temporal-Difference
HW	Hardware
SW	Software
ADC	Analog-Digital Converter
SPI	Serial Peripheral Interface
PWM	Pulse-Width Modulation
CSV	Comma-Separated Values
CNS	Central Nervous System
DMA	Direct Memory Access
UART	Universal Asynchronous Receiver-Transmitter
MEMS	Microelectromechanical systems
PPG	Photoplethysmogram
BLE	Bluetooth Low Energy
AI	Artificial Intelligence
DOF	Degrees of Freedom
IMU	Inertia Measurement Unit
CRC	Cyclic Redundancy Check

1 Introduction

Nowadays, a huge amount of the wheeled devices exist around us. Industrial carts and transporters are used in nearly every industry and warehouse. Over decades, a number of studies have shown that the use of manual vehicles improves human efficiency and decreases the stress level in manual handling tasks [1] ,[2], [3], [4].

In this work the complex approach to the study of human-mobile cart interaction was applied. The topic itself brings together physics, control theory, the emotional side of human being such as pleasure or comfort and reinforcement learning. This work contributes to different levels from information collection to hardware development and statistical analysis.

The thesis consists of twelve parts. The first part is introduction that describes the thesis content and explains how to navigate through the work. In the second part the problem statement is defined. By analysis of world statistics the weak points material handling process were collected. Known risk factors, topic relevance and demand as well as their root causes were evaluated. Current state of the art in the area of human-cart interaction was described in the part three. In the fourth part author's motivation to carry out the research is formulated. To find out more about the research objectives and design of the research project, please follow the chapter for more details.

Methods used in this work were presented in chapter 6. Chapter 7 reviews the process of the test platform development including the main requirement HW design, SW implementation, description of cart kinematics and dynamics. Chapter 8 presents the workflow of human-operator study starting with the description of the human motion and following description of applied methods for evaluation of the operator's feedback.

Chapter 9 describes the process of human - industrial cart interaction. It includes analysis of raw data and experiment design. In the chapter 10 regression analysis of the experiment results is performed in order to find dependencies between measured physical values from industrial cart and emotional feedback from the operator.

Chapter 11 reinforcement learning demonstrates the implemented algorithm that uses rating system based on actions, states and rewards. Based on the rewards the learning system gets for the actions, algorithm could change the system state and adjust impedance controllers according to the intentions of the operator.

Thesis is concluded by the collection of outcomes and technical solutions, highlights of the thesis, as well as suggestions for possible future research opportunities and the area of human-industrial cart interaction.

2 Problem statement

> "If you define the problem correctly, you almost have the solution."
>
> Steve Jobs

In this chapter the statement of the problem is formulated and later resolved in the workflow of the thesis. Starting with the world statistics overview, it would be possible to estimate an effect of human-cart interaction problem. In the following steps we collected the information about the factors that could affect the interaction process and lead to injuries or hazards. Possible injuries and hazards are joined up in a system. The problem that is addressed by the thesis is formulated in the following pages.

Industrial cart manipulation is a physical activity of a human operator that involves exertion of considerable force in order to overcome the forces that resist motion and reach target position. When operator carries a loaded or empty industrial cart, he generates force and transmits that force through a contact points to the cart. Previous researchers [5] have identified a number of key factors that have a great effect on the human – cart interaction process during manual pushing and pulling tasks. The key factors for pushing/pulling task are shown in the figure 2.1.

Figure 2.1: Key factors for pushing/pulling task from [5]

Several studies have reported a relationship between pushing/pulling and shoulder pain, such as increased shoulder pain from pushing/pulling wheeled equipment

[6]; pushing/pulling heavy weights [7] and pushing against a high handle [8].

A review and provided recommendations about maximum acceptable pushing and pulling forces was developed by Garg et al. [9]. Cross-sectional epidemiological studies show that cart manipulation activities are associated with shoulder and low-back pain and musculoskeletal disorders [10] and [11]. Pushing and pulling of carts and objects exposes workers to two types of hazards: stresses to the musculoskeletal system from applied hand force, and (ii) accidents due to slipping or tripping [12].

Pushing, pulling, and maneuvering hand carts involves some common hazards (overexertion). The most common injuries that result from hand cart operations are:

- fingers and hands being caught in, on, or between the cart and other object
- toes, feet and lower legs being bumped into or crushed by the cart
- slips, trips, and falls, and strain injuries predominantly for the lower back, shoulder, and arm muscles and joints

The size-weight illusion (SWI) describes the phenomena of underestimation or overestimation of the required effort when moving or lifting the loads. SWI effect often happens to inexperienced operators. However, even experienced users may belong to the risk-prone group. Underestimation of SWI effect may lead to injures described in the section 8.2.

2.1 Topic relevance

Manual cargo transportation tasks, many of which require pushing, pulling and rotating are common in almost all industrial and warehouse environments. Nearly half of all manual materials handling consists of pushing and pulling activities [14]. This work focuses specifically on carrying activities while using industrial power assisted carts. These tasks expose workers to musculoskeletal stresses as well as other related injuries, slipping and tripping hazards. Many big companies (Wanzl, TGW, Siemens etc.) offering solutions for industrial and warehouse logistic are interested in the research conducted to improve the productivity, efficiency and work safety.

Material handling exposes the worker to known risk factors for low-back disorder, such as lifting, bending, twisting, pulling, pushing and maintenance of static postures.

If we take a look at the fatal and non-fatal accidents statistics in Europe in 2013 according to the Eurostat information that shown in the figure 2.2, it becomes clear that first three activities are the most dangerous.

People who work in construction, transportation and manufacturing suffer from many injures. Nearly 40% of all non fatal injures come from this three activities. 54% all deaths during working hours also happen in construction, transportation and manufacturing. Risk factors related to transportation and manual handling tasks are placed second in the graph 2.3 of fatal and non-fatal accidents at work.

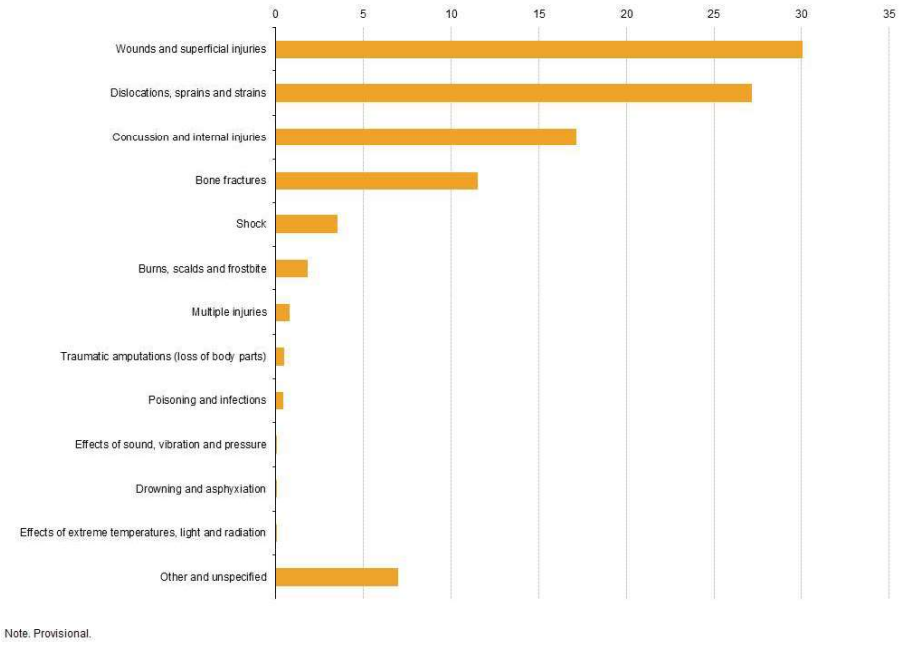

Figure 2.2: Fatal and non-fatal accidents statistics in Europe in 2013 [13]

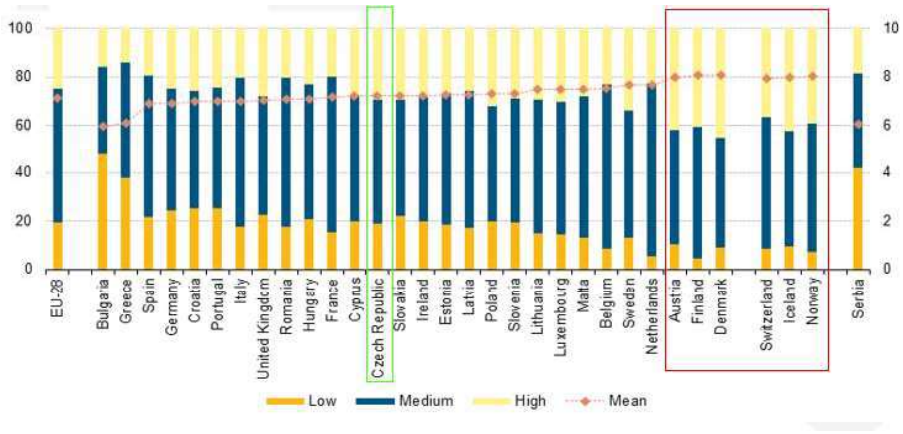

Figure 2.3: Fatal and non-fatal accidents at work by type of injury in 2013 [13]

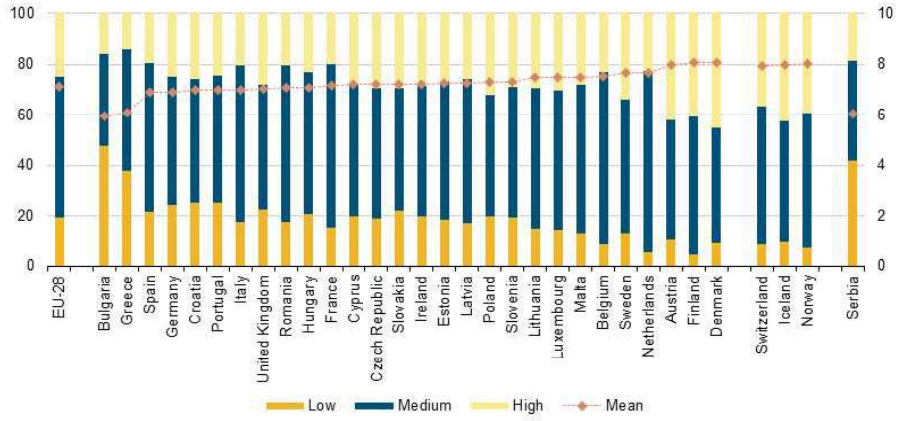

Figure 2.4: Satisfaction with job in the industry, by country in 2013 [13]

If the job satisfaction level is analyzed, it is demonstrated in figure 2.4 that people in the countries that pay a great attention to human-robot interaction and the use of robotic systems are happier and more satisfied with their jobs and lives.

Existing statistics do not reflect the importance of maneuvering with industrial cart as work factors causing injury in the full scope, because the injuries fall into different categories making them difficult to analyze.

3 State of art

> "A state-of-the-art calculation requires 100 hours of CPU time on the state-of-the-art computer, independent of the decade."
>
> Edward Teller

The objective of this chapter is to review the existing information on human – mobile robot physical interaction including hazards, problems and existing solutions in the area of psychophysics, ergonomics, physics and automation control theory.

When analyzing the state of the art in the field of human – robot physical interaction, it is necessary to consider the problem from the point of physical interaction between the human-operator and industrial cart, and the methods of emotional feedback evaluation during his interaction with the cart. This chapter shows the most promising power assisted techniques developed by previous researchers, as well as the works related to the evaluation of operator's characteristics.

The subject of chapter one is the demonstration of existing theories and approaches in the field of power-assisted vehicles. This topic is quite relevant nowadays, as in the last few decades there have been a large number of studies related to the physical human-robot interaction (between a man and a machine).

Currently, there are several ways to control the power assisted vehicle:

1. Impedance/Admittance control
2. Compliance control
3. Model Reference Adaptive Impedance Control (MRAIC)
4. First order lag controller

Last but not least, laws and standards like the DIN EN ISO 10218-2 [15], enable and promote a closer interaction between humans and robots.

A great deal of research has been done on physiological and psychophysical aspects of materials handling. Ciriello and Snook [16],[17] have published a large data base for designing lifting, lowering, pushing, pulling and carrying tasks. [18] study the maximum comfortable forces for pushing and pulling a cart. In addition, there have been many contributions to the human-robot physical interaction area related

to impedance and compliance control [19], [20], force/motion impedance control [21], model reference adaptive impedance control [22]. In parallel, adaptive control of robotic manipulators has advanced considerably in recent decades to reduce dependency on a precise knowledge of the dynamics of the robot and the environment. This has led to works on adaptive impedance control [23], [24].

The previous study focused on design factors of carriers and their effects through kinematical and biomechanical models. Despite their effort on the carrier design improvement in terms of human factors, there are still various injuries because users' preferences and reactions were not considered in the studies.

This dissertation gives a systematic approach in development of a unified, flexible and inexpensive device developed for comfortable human-robot interaction that responds to the human operator expectations. The use of hand carts to transport loads instead of carrying them saves workers a lot of effort. It decreases the risk of overexertion injury in jobs that include manual materials handling.

3.1 Impedance/Admittance control

Theoretical concept of Impedance control was firstly introduced in 1985 by Professor Neville Hogan from Massachusetts Institute of Technology (MIT) [20]. The objective of impedance control is not to directly control position or force, but the relationship between them. This allows to reduce or increase apparent stiffness, damping, or mass depending on the task. The overall purpose of the impedance control creation was to develop an approach to control a manipulated object that would be suitable for a broad range of applications. General impedance control scheme is shown in the figure 3.1.

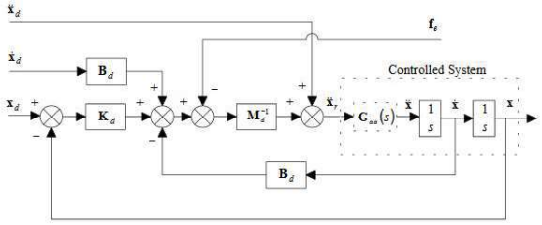

Figure 3.1: Block diagram of an impedance controller form [21]

Manipulation with the object of interest requires a physical interaction. In order to fulfill the task requirements, the user chooses a desired impedance that could be expressed by the following equation 3.1:

$$M_d(\ddot{x} - \ddot{x_d}) + B_d(\dot{x} - \dot{x_d}) + K_d(x - x_d) = -f_e \tag{3.1}$$

Where M_d, B_d and D_d are positive constants that represent the desired inertia, damping and stiffness, respectively. From the equation 3.1 we could find the

acceleration reference described by 3.2:

$$\ddot{x_r} = \ddot{x_d} + M_d^{-1}[-f_e + B_d(\dot{x} - \dot{x_d}) + K_d(x - x_d)] \tag{3.2}$$

For admittance control, the control force is a position-controller designed to track the trajectory $x = x_d$. Trajectory tracking is implemented using a PD controller with positive gains K_p and K_d:

$$f_r = K_p(x_d - x) + K_d\dot{x} \tag{3.3}$$

The simplified impedance controller could be written in the following form:

$$M_d(\ddot{x} - \ddot{x_d}) + B_d(\dot{x} - \dot{x_d}) = -f_e \tag{3.4}$$

It was proved by previous researchers [24] that the spring component of the impedance controller does not have a significant impact on the process of interaction.

The impedance controller is a virtual dynamic system. Along with the compliance controller it allows to set any desired system dynamics. By changing the settings of the virtual mass (Mass), a virtual damper (Damp) and virtual spring component we can obtain the desired system response to the control impact. In our work we will use two controllers. One controller will be used for translation motion in support of pushing and pulling tasks. The second controller will be used for rotational motion in order to support the human operator in the task of rotation.

3.2 Compliance control

The example of power – assisted control based on compliance controller was proposed by A. Nagami et al [19]. The author expresses his opinion regarding the conditions that should be taken into account by the operator when moving loads. The main idea of his work is the implementation of the operator's desired movement without the influence of external disturbances.

Compliance controller makes it possible to perform the assist motion for the cart operator smoothly and improve the stability of the cart motion. The compliant controller with variable gain is shown in figure 3.2.

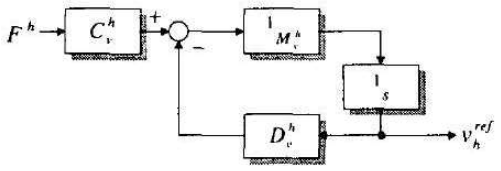

Figure 3.2: Block diagram of the compliant controller based on the applied force by A. Nagami et al [19]

The variable compliant gain, and is adjusted so that the cart operator can move the platform smoothly independently of the loaded object. The variable compliant

gain formula is expressed by the equation 3.5:

$$C_v^h = \tan(a_v^h F^h) \tag{3.5}$$

where F^h - human force, a_v^h - adjustable coefficient.
Compliance controller speed reference is listed in 3.6:

$$\dot{v_h}^{ref} = \frac{1}{M_v^h}(C_v^h F^h - D_v^h v^h) \tag{3.6}$$

The parameters of the compliance controller are chosen empirically, which does not allow to apply the developed solution for mobile carts with modified parameters without prior resetting.

3.3 Model Reference Adaptive Impedance Control (MRAIC)

Model Reference Adaptive Impedance Control (MRAIC) allows not only to track the response of the reference model but also to make the dynamics of the closed-loop system similar to the reference impedance model.

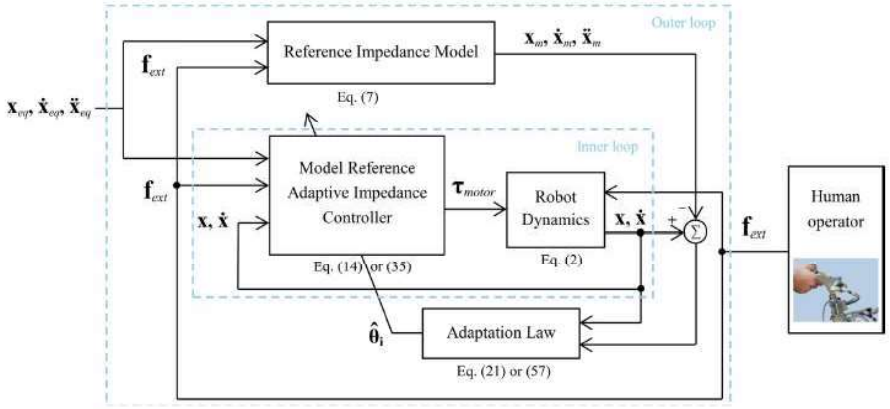

Figure 3.3: The structure of the Model Reference Adaptive Impedance Controllers [22]

The desired reference impedance model for the robot end-effector in Cartesian coordinates is generally defined by the equation 3.7. The reference model has two poles in each Cartesian coordinate direction as:

$$r_1 = -\lambda_1 + i\lambda_3 \tag{3.7}$$

$$r_2 = -\lambda_2 + i\lambda_3 \tag{3.8}$$

where for the reference model stability, constants λ_1 and λ_2 should be positive.

The model reference adaptive impedance controller for motor torque could be written in the following form:

$$\tau_{motor} = \hat{M}_q v_1 + \hat{C}_q v_2 + \hat{G}_q + \hat{F}_q - J^T f_{ext} \tag{3.9}$$

where v_1 and v_2 are known vectors that do not contain any estimated parameters of the robot's dynamics.

$$v_1 = J^{-1}\left(\ddot{x_{eq}} - \frac{c}{m}(\dot{x} - \dot{x_{eq}}) - \frac{k}{m}(\dot{x} - \dot{x}_{eq}) + \frac{1}{m}f_{ext} + {\lambda_3}^2\tilde{x} - \dot{J}J^{-1}\dot{x}_r\right) \tag{3.10}$$

$$v_1 = J^{-1}\dot{x}_r \tag{3.11}$$

Linearly parameterized equation in joint space has the following formula:

$$\tau_{motor} = Y_1\hat{\theta}_1 - J^T f_{ext} \tag{3.12}$$

where $\hat{\theta}_1$ -estimation of actual parameters vector, Y_1 - regressors matrix in joint space.

$$Y_1\hat{\theta}_1 = M_q v_1 + C_q v_2 + G_q + F_q \tag{3.13}$$

The adaptation law is expressed by the equation 3.14:

$$\dot{\hat{\theta}}_1 = -\Gamma Y_1^T J^{-1} s_1 \tag{3.14}$$

where Γ is symmetric positive definite matrix. s_1 is error dynamics.

$$s_1 = \dot{x} - \dot{x_{eq}} \tag{3.15}$$

where $\dot{x_{eq}}$ is the reference velocity.

$$\dot{x}_r = x_m - \lambda_1\tilde{x} \tag{3.16}$$

$\tilde{x}$ is the reference model position error. This method gives very promising results. However, it requires reference impedance model that is not available in our case due to the human factor.

3.4 First order lag controller

Power-assisted control based on the first order lag controller and fuzzy logic was introduced in the work of K. Terashima et al [25] called "Auto-tuning Control of Power Assist System Based on the Estimation of Operator's Skill Level for Forward and Backward Driving of Omni-directional Wheelchair". Block diagram of skill assist system is shown in the figure 3.4.

In this work the author demonstrates his own developed methods to assess the level of operator's competence and configuration of a power – assisted controller using fuzzy logic. It is demonstrated in the figure 3.5.

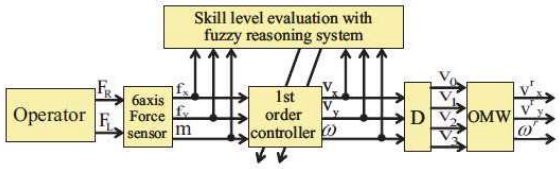

Figure 3.4: Block diagram of skill assist system by K. Terashima et al [25]

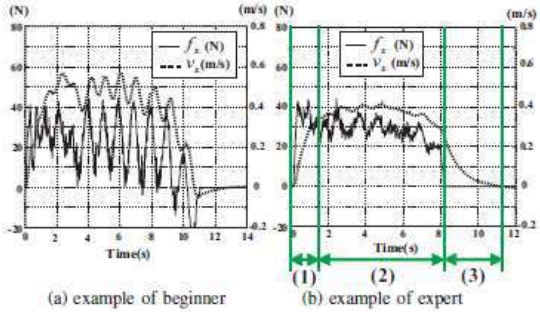

Figure 3.5: Skill level estimation K. Terashima et al [25]

The author mentions that the developed system has a difficulty with adding support in rotational motion. Operator feels uncomfortable during the manipulation and fluctuations in the support system when vibration is caused by the operator force. For this reason, this paper considers the support for the backward and forward movement. First-order lag controller is used in order to convert the force applied by the operator's into the motor speed setpoint. The controller formula:

$$\begin{bmatrix} v_x \\ v_y \\ w \end{bmatrix} = \begin{bmatrix} \frac{k_{vx}}{T_{vx}s+1} & 0 & 0 \\ 0 & \frac{k_{vy}}{T_{vy}s+1} & 0 \\ 0 & 0 & \frac{k_{vz}}{T_{vz}s+1} \end{bmatrix} \begin{bmatrix} f_x \\ f_y \\ m \end{bmatrix} \tag{3.17}$$

Performance index evaluating operator's skill degree:

$$\sigma_{vx} = \sqrt{\frac{1}{n}\sum_{i=1}^{n}(v_{xi} - \bar{v}_x)} \tag{3.18}$$

Skill level index:

$$S_{vx(t)} = S_{vx(t-1)} + \frac{\sigma_{vxs}}{T_s} \tag{3.19}$$

where T_s – forgettable time.

The author conducted a comparative experiment for two people and has proposed a formula to evaluate the skill of the operator. Later he conducted another experiment for four people and confirmed the correct operation methods for the operator's evaluation and the regulator setting when moving backward and forward. The implementation of presented methods for lateral, rotational and slant movement was suggested for further research.

3.5 Aspects of human comfort and expectations

Aspects of human comfort and expectations during human – industrial cart interaction are poorly studied. There are no studies related to the human comfort estimation during goods transportation process with help of IPAC. However, L. A. Silva presents a cart built to move 500 kg net loads with friendly human perception [26]. The complete system is shown in the figure 3.6.

Figure 3.6: Mechanical traction system for electrical load cart developed by L. A. Silva et al [27]

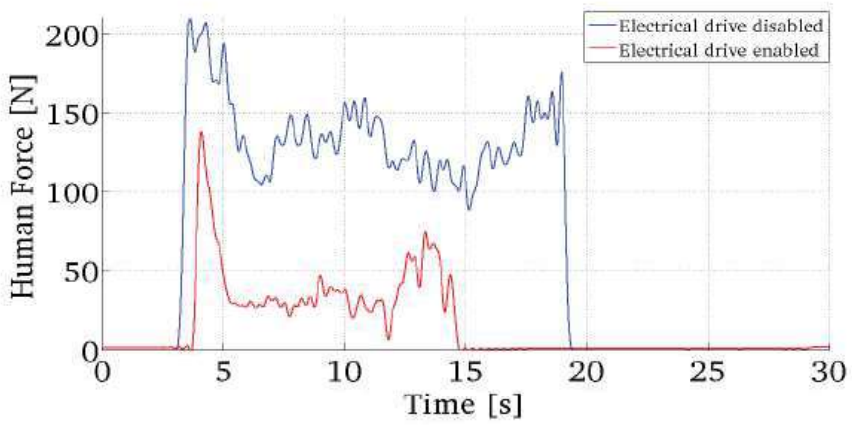

Figure 3.7: Human force with 120kg total load over a non-inclined surface [27]

In his study, the mechanical structure and power elements were designed to aid in translational displacements of 500kg net load. The human command were measured by a 1300N side effort compensated load cell.

The control system developed by L. A. Silva is based on emulated mechanical impedance that generates the speed setpoint. The block diagram of the control system is shown in the figure 3.9.

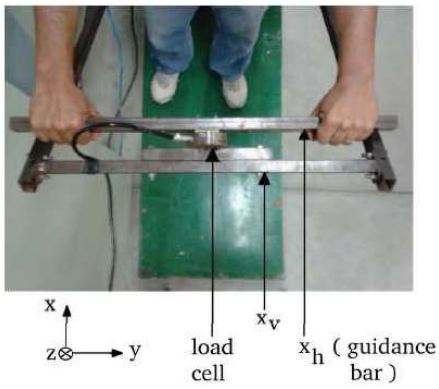

Figure 3.8: Load cell mounting scheme for human force measurement [27]

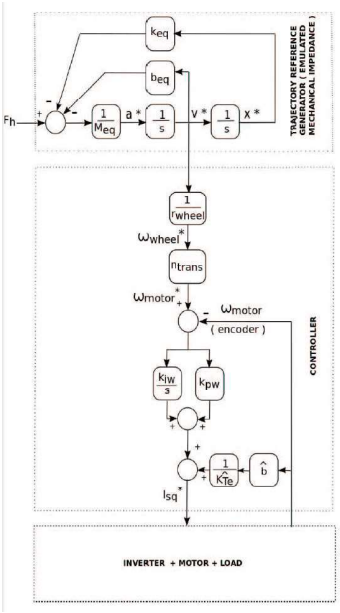

Figure 3.9: Control system block diagram purposed by L. A. Silva et al [27]

In order to evaluate the force controller performance, author compared the human force necessary to move the vehicle when the human aid system was enabled or disabled. As shown in figure 3.7 the average human force necessary to move the cart without help from the cooperative system is about 3.5 times greater than that observed when the system is enabled.

4 Motivation

In our work we would like to evaluate a new power assistance system with human comfort estimation, which sets up operator's pushing, pulling and rotational force to the comfortable level and decreases the risk of injury. One of the highlighted specific challenges of the research was to develop a cart that responds more flexibly, robustly and efficiently to the everyday needs of workers and citizens in professional or domestic environments.

The motivation for this research is to reduce the number of injuries of people who work in the area of material handling by solving the problem of faulty interaction between human-operator and industrial cart. It is proposed to establish the system that recognizes and adapts to the human-operator intentions based on rewards and losses received for the quality of interaction process.

One significant part of the research is to specify the requirements for the industrial cart, develop the proper mechanical design and equip the cart with required set of sensors. Another important part is to design the architecture of the control system and implement the elements of artificial intelligence that affect the interaction process.

The plan is to have the state, where the industrial cart responds to the human-operator intention with required dynamics. As a result, human oriented study has to be performed. It is necessary to find the correlation between emotional feedback of the human operator and physical measures that could be obtained using sensors of industrial cart.

In order to have a good overview on independent variables that affect human-operator comfort, interaction process parameters have to be collected and evaluated using regression analysis. Using questionnaire based technique the emotional feedback of the human operator will be obtained. The effect of found variables will be evaluated with the group of experienced and inexperienced human-operators.

Based on this dependency the reward system will be defined. Using the methods of artificial intelligence support system will adapt to the human operator intention by switching between different states and getting rewards for each single action. In the end the set of impedance controller parameters will be selected based on the highest value of the interaction process quality for particular operator. It leads to adaptation of industrial cart dynamics according to the intention of the human operator.

5 Goal and Objectives

The key point of the comfortable human – industrial cart physical interaction is the question how to include physiological and psychophysical aspects of the human operator in to the control system. Furthermore, as far as the author is aware, no estimation criteria for operator's comfort level and subjective expectations from the interaction process have been developed to this day.

The research goal is to find proper mechanical design and methods of intelligent control in order to achieve a state where an operator can manipulate a heavy loaded industrial cart with minimum physical effort and ultimate comfort. Processing of measured forces at the human-cart interface with recognition of the desired behavior and following calculation of the control impact for electric drives is assumed.

In order to achieve the goal, the following objectives are apparent:

1. Collect the state of art information in the area of physical human-robot interaction and the most promising existing algorithm that can be adapted to deliver a new human-powered cart interaction control technique through literature analysis and practical investigations.

2. Prepare a mathematical description for dynamics and kinematics of the human – cart physical interaction model.

3. Develop and assemble an experimental model of an industrial cart.

4. Perform a set of experiments including real people and estimate the human feedback during the interaction process.

5. Analyze dynamic characteristics in order to search for criteria that directly or indirectly determine a physical feeling of human comfort and his expectations during the interaction with IPAC.

6. Synthesize the human estimation criteria that characterize the satisfaction and comfort from the human- powered cart interaction process.

7. Develop the human – powered cart interaction control algorithm based on the synthesized criteria.

8. Verify the work of purposed solution for the developed industrial cart.

6 Methods

In this chapter we describe the way we would like to reach the goal and meet objectives defined in the beginning of the research. Theoretical, empirical and mathematical research methods are combined in this work in order to reach the goal formulated in chapter 5. The methods and objectives sorted by the research type and addressed by the current study are listed below.

Theoretical methods:

- Analysis and synthesis of existing information was performed to determine the state of the art and current research gaps.
- Modeling was used for industrial cart simulation and development of kinematic and dynamic models.

Empirical methods:

- Observation was used to detect interaction states and conditions that could have a positive or negative effect on the feelings of the cart operator.
- Survey was used to collect the feedback from human operators after the interaction process.
- Experiment was used to collect the data of the interaction process with changing conditions such as impedance controller settings, loads and operators.

Mathematical methods:

- Statistics method - regression analysis was performed to evaluate the experimental data and determine the dependency between human operator feedback and measured parameters of the interaction process.
- Programming was used to implement control algorithm.

7 Test platform development

7.1 Main requirements

This section describes the main requirements for a mobile platform that was created for testing and verification of operator's comfort. This developed model consists of aluminum profile, the basis of the platform is set on the four cluster wheels. In the center of the platform there are two leading wheels that function according to the principle of differentiated drive.

The vehicle has been constructed to suit the following parameters:

- to be easy-assembled, cheap, rapid prototyping oriented
- to allow measurement of human-vehicle interaction characteristics
- to hold the maximum load mass in the range of 500 kg
- to attain the speed of the walking human in a range of 5 km/h

7.2 Hardware design

The developed platform has the characteristics shown in the table 7.1.

N	Parameter	Value
1	Length	1.255 [m]
2	Width	0.8 [m]
3	Height	1.275 [m]
4	Mass	53.535 [kg]
5	Max. Load	500 [kg]
4	Max. Speed	5 [km/h]

Table 7.1: Cart parameters

System actuators are presented by two 350W motors MY1016Z connected to the wheels via chain belts. The drive is shown in the figure 7.3.

In the back of the trolley there is a handle for the operator. The handle is connected to the body of the trolley through the tensiometers, which are located on the right and left side of the trolley. For detailed information please see the visual 7.2.

Figure 7.1: Test platform [28]

N	Parameter	Value
1	Power	350 [W]
1	Voltage	24 [V]
2	Current	18 [A]
3	Rotor Resistance	1.3 [Ohm]
4	Rotor Inductance	0.001 [H]
5	kV	500 [kg]
4	Max. Speed	5 [km/h]

Table 7.2: Motor parameters

N	Parameter	Value
1	Excitation	10 [Vdc]
2	Load	±100 [KgF]
3	In Resist	378.3 [Ohm]
4	Out Resist	351.9 [Ohm]
5	Sensitivity	2.9994 [mV/V]

Table 7.3: Tensiometer parameters

The leading wheels are connected to the drives by a chain belt. The drives are accommodated with encoders. In the chain of anchors of each drive there is a current sensor.

Selected motors are equipped with $z_m = 9$ teeth pitch 12.7 roller. The desired linear speed of the powered cart $v_d = 5[km/h] = 1.389[m/s]$. Powered wheel diameter $D_w = 200[mm] = 0.2[m]$. Desired wheel rotational speed [rpm]:

$$n_w = \frac{60\ v_d}{\pi\ D_w} = (60 \cdot 1.389)/(3.14 \cdot 0.2) = 132.696 \tag{7.1}$$

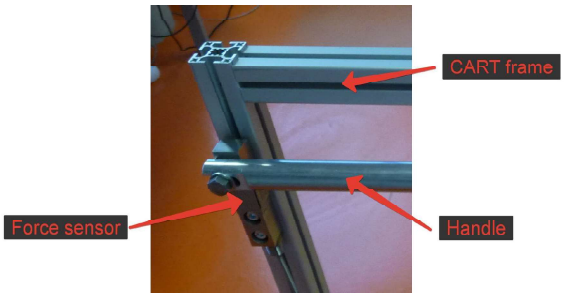

Figure 7.2: Tensiometer location

Gear ratio:

$$G_r = \frac{n_m}{n_w} = 353/132.696 = 2.66 \tag{7.2}$$

Teeth number of the wheel gear:

$$z_w = G_r \cdot z_m = 2.66 \cdot 9 \approx 24 \tag{7.3}$$

Final overview of the developed drive system is shown in the figure 7.3.

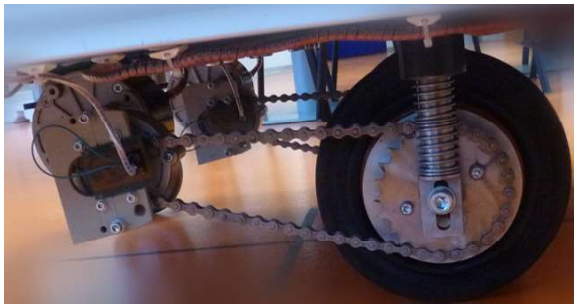

Figure 7.3: Drive system

Motor control is carried out with the help of a driver. The driver is controlled by a controller of a lower level. The controller of a lower level collects and partly processes the signals from peripheral areas (encoders, current sensors, tensiometers). The lower level controller is also connected to the extra controller that is responsible for collecting and processing the data from IMU (magnetometer, accelerometer and gyroscope).

Detailed description of the technical characteristics could be found in the technical specifications [29], [30], [31], [32].

The second revision of the hardware consisted of HX711. Tensiometers are processed by a pair of 24bit analog-to-digital converters HX711.

Inertia measurement unit is presented by HMC5983 and MPU6050. HMC5983 is a temperature compensated three-axis integrated circuit magnetometer and MPU6050 is combining a MEMS 3-axis gyroscope and a 3-axis accelerometer.

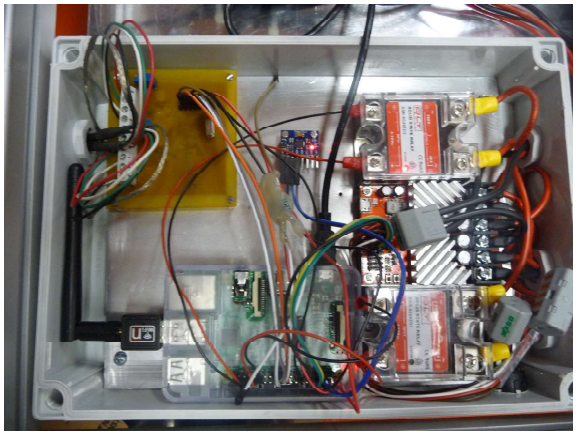

Figure 7.4: Control system hardware Rev.1

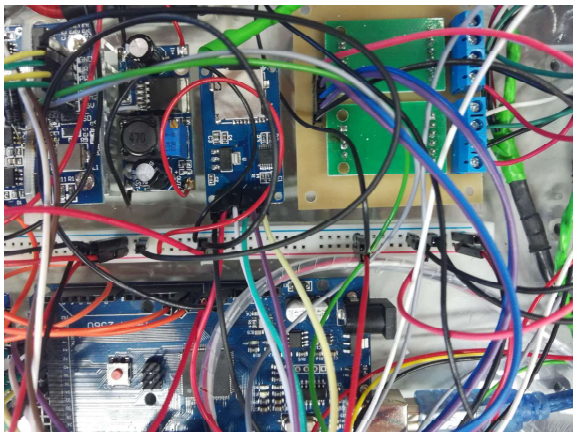

Figure 7.5: Control system hardware Rev.2

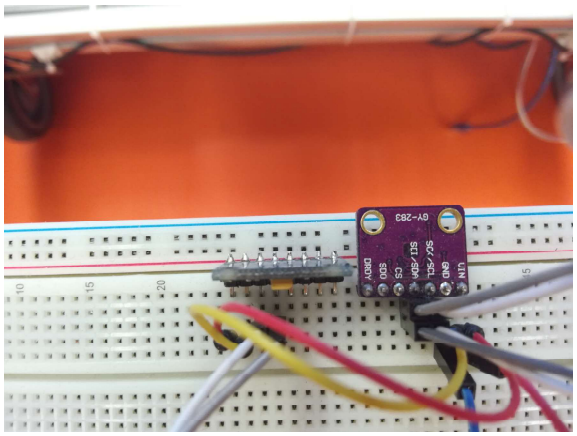

Figure 7.6: Inertial measurement unit (IMU)

7.3 Software development

In order to extend the number of ready-made modules and to decrease the time spent on programming and manuals, it was decided to merge libraries from ARDUINO open-source community with Matlab Simulink. To use the original Wiring language of ARDUINO with RPi, the Wiring Pi library was developed. To ensure that the Matlab compiler could use the library functions we need to add the link to the compiler settings that emerge via Xmakefilesetup.

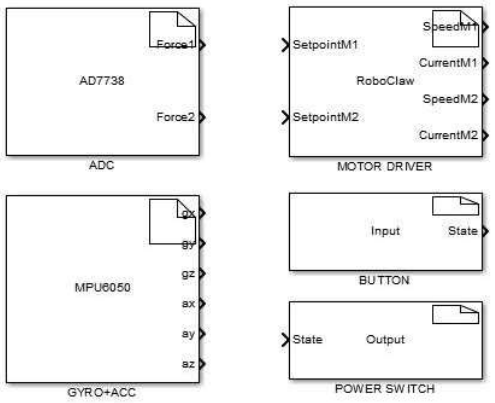

Figure 7.7: Developed Matlab blocks

7.4 Cart kinematics

The vehicle used in this paper has two driving wheels and four passive casters. The IPAC model used in this paper is shown in the figure 7.8. To simplify the kinematics model of the vehicle, it is assumed that casters are not active.

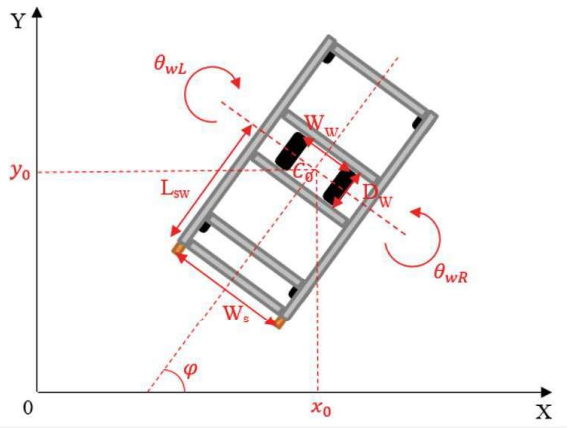

Figure 7.8: Cart kinematics

Parameters shown in the figure 7.8 have the following description: W_s – distance between two sensors; W_w – distance between two wheels; L_sv – distance between sensors installation line and wheels installation line; ${}_wL$, ${}_wR$ – wheels rotation angles; – direction angle; x_0 , y_0 – position of the vehicle in the world coordinates; C_0 – the middle point between the two powered wheels. Mathematical description of the control object is presented below.

Relation for linear and angular velocity:

$$v = wR \tag{7.4}$$

Relation for linear and angular velocity:

$$v_{\sum cart} = \frac{D_w}{4} \left(w_{wheel\_left} + w_{wheel\_right}\right) \tag{7.5}$$

Velocity at $C_0(x_0, y_0)$ point is described by the equations 39 and 40 (Conversion from polar to Cartesian coordinate system).

$$\dot{x_0} = v_{\sum cart} \cos(\phi) \tag{7.6}$$

$$\dot{y_0} = v_{\sum cart} \sin(\phi) \tag{7.7}$$

Dependency of powered cart angular velocity from angular velocity of the wheel:

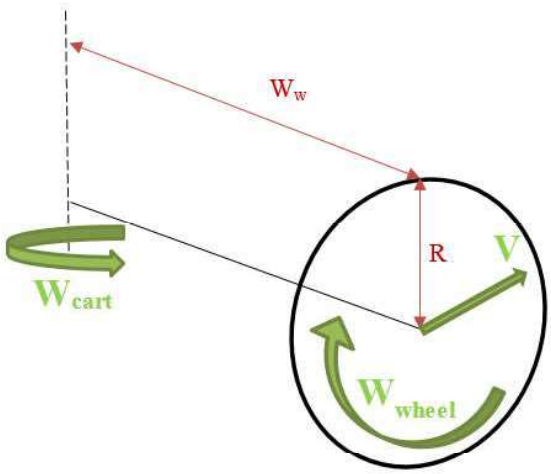

Figure 7.9: Angular speed conversion

Wheel linear velocity:

$$v = w_{cart}L = w_{wheel}R \tag{7.8}$$

Cart angular velocity generated by one wheel:

$$w_{cart} = w_{wheel} \frac{R}{L} \tag{7.9}$$

Cart angular velocity at the point C_0:

$$w_{\sum cart} = \frac{D_w}{2W_w} \cdot (w_{wheel\_left} - w_{wheel\_right}) \tag{7.10}$$

Matrix form of the equations 7.5 and 7.9 is shown in 7.10. Control vector is defined as $\dot{X} = [v_{cart\_sum}, w_{cart\_sum}]^T$, rotational speeds vector is defined as $\dot{\theta} = [w_{wheel\_left}, w_{wheel\_right}]^T$.

$$\dot{X} = \begin{bmatrix} v_{\sum cart} \\ w_{\sum cart} \end{bmatrix} = \begin{bmatrix} \frac{D_w}{4} & \frac{D_w}{4} \\ \frac{D_w}{2W_w} & -\frac{D_w}{2W_w} \end{bmatrix} \times \begin{bmatrix} w_{wheel\_left} \\ w_{wheel\_right} \end{bmatrix} = J_{aco} \cdot \dot{\theta} \tag{7.11}$$

By differentiating the equation 7.11 we obtain an equation for the total linear and angular acceleration:

$$\ddot{X} = J_{aco} \cdot \ddot{\theta} + J_{aco} \cdot \dot{\theta} \tag{7.12}$$

The second term on the right side has a insignificant impact on the acceleration value compared to the first term and could be neglected.

$$\ddot{X} = J_{aco} \cdot \ddot{\theta} \tag{7.13}$$

In order to obtain equation for calculating the wheel angular accelerations, we need to find the pseudo-inverse matrix J_{aco}^{-1*}.

$$\ddot{\theta} = J_{aco}^{-1*} \cdot \ddot{X} \tag{7.14}$$

$$\begin{bmatrix} \varepsilon_{wheel\_left} \\ \varepsilon_{wheel\_right} \end{bmatrix} = \frac{D_w}{4} \cdot \begin{bmatrix} 1 & \frac{W_w}{2} \\ 1 & -\frac{W_w}{2} \end{bmatrix} \begin{bmatrix} a_{cart\_sum} \\ \varepsilon_{cart\_sum} \end{bmatrix} \tag{7.15}$$

Based on the kinematic model, we can determine the position and direction of movement of the industrial trolley from the rotation speed of the left and right wheels. This dependence is presented in the form of MATLAB diagrams in the figure 7.10.

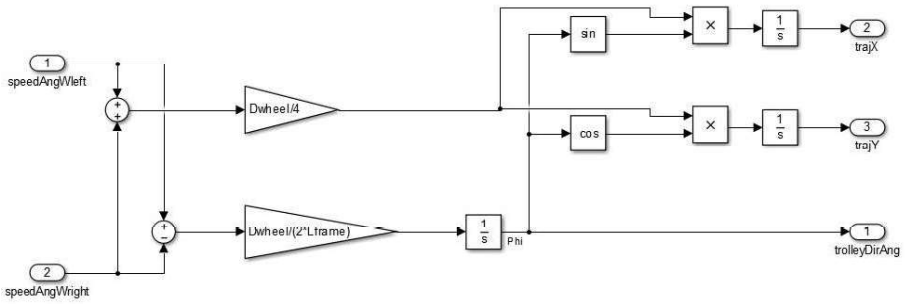

Figure 7.10: Industrial cart kinematics

The angular velocity of the wheels could be derived based on the linear and angular velocity of the cart according to the equations 7.16 and 7.17.

$$w_{wheel\_left} = \frac{2v_{cart} + W_w w_{cart}}{D_w} \tag{7.16}$$

$$w_{wheel\_right} = \frac{2v_{cart} - W_w w_{cart}}{D_w} \tag{7.17}$$

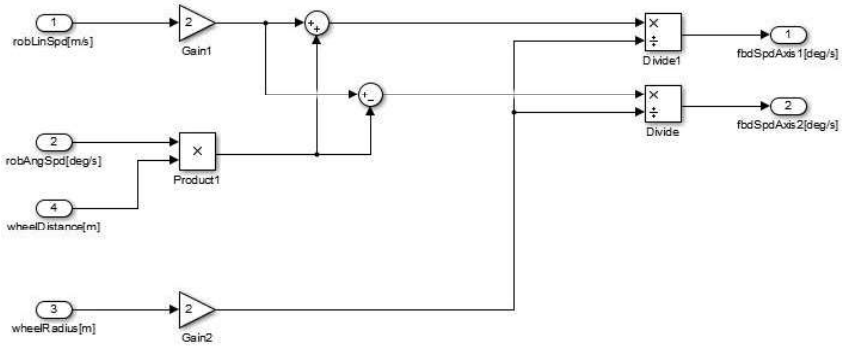

Figure 7.11: Matlab diagram for velocity conversion

7.5 Human operator interface

As it was mentioned in the chapter 7.2 the cart is equipped with two tensiometers. They are shown in the figure 7.12. The handle is connected to the cart body through them. These tensiometeres are used to measure interaction forces and torques for transnational and rotational motions correspondingly. They can measure the force along one axis (push and pull motions), but it allows operator to control all DOFs because the cart has only 2DOF (one rotational and one translational degree). The operator plans a handling task based on his own desires and expectations as well as information from his sense organs (vestibular and vision systems), and provides the information about the motion to the cart by acting on the handle. Forces detected on the left and right sensors are resolved into translational force and rotational torque in the cart coordinates.

Transnational force for the motion in linear direction could be written as a simple sum of the measured force values as described by the equation 7.18.

$$F_{\sum h} = F_{hr} + F_{hl} \tag{7.18}$$

Equation 7.19 presents a rotational torque for the motion around the axis that goes vertically through the central point C_0. See figure 7.8 for more details.

$$T_{\sum h} = (F_{hr} + F_{hl}) \times \sqrt{(W/2)^2 + (L/2)^2} \tag{7.19}$$

where W is the width of the cart and L is the cart length. Values for cart length and width could be found in table 7.1.

Figure 7.12: Handlebar for pHRI

7.6 Cart dynamics

In order to build the dynamic model we will use the equations of Newton-Euler, describing the system from the point of view of all forces and moments that influence the system. This method is a direct interpretation of Newton's Second law.

Let J be the moment of inertia towards the Central vertical axis and m is the mass of the industrial trolley with the differential drives Using Lagrange's equations we obtain the following mathematical model:

$$\begin{bmatrix} m & 0 & 0 \\ 0 & m & 0 \\ 0 & 0 & J \end{bmatrix} \times \begin{bmatrix} \ddot{x} \\ \ddot{y} \\ \ddot{\theta} \end{bmatrix} = \begin{bmatrix} F_x \\ F_y \\ M_\theta \end{bmatrix} = \begin{bmatrix} cos\theta & 0 \\ \sin\theta & 0 \\ 0 & 1 \end{bmatrix} \times \begin{bmatrix} F \\ M_\theta \end{bmatrix} \tag{7.20}$$

Given the strength of the Coriolis and centripetal acceleration we can write this model in the following form:

$$m\ddot{x} - m \cdot v_y \cdot w = F_x \tag{7.21}$$

$$m\ddot{y} - m \cdot v_x \cdot w = F_y \tag{7.22}$$

$$J\frac{dw}{dt} = M_\theta \tag{7.23}$$

where $F_x = F \cdot sin\theta$, $F_y = F \cdot cos\theta$, $v_x = v \cdot sin\theta$, $v_y = v \cdot cos\theta$, $v = \sqrt{v_x^2 + v_y^2}$

Dynamic model of the industrial cart is shown in the figure 7.13. DC motors are widely used in power assisted devices and are one of the major actuators used in mobile robotics. We implement the model of the drive to create detailed dynamic models of the system. A control system block diagram of the engine is shown in the figure 7.14. After the macroblocks of the main elements of the model are created, we obtain a complete Simulink model of an industrial cart. The model is shown in the figure 7.15.

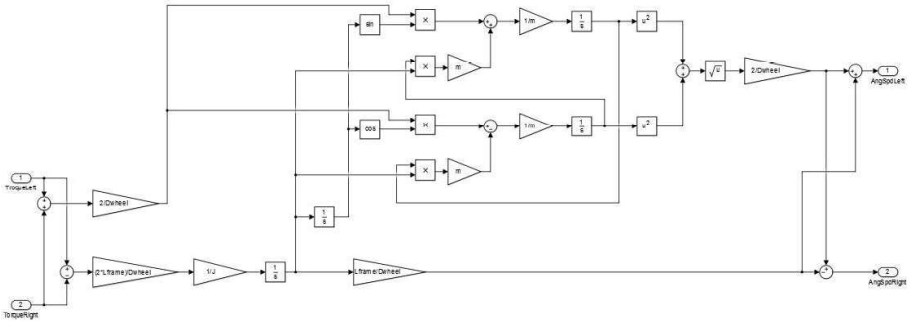

Figure 7.13: Industrial cart kinematics

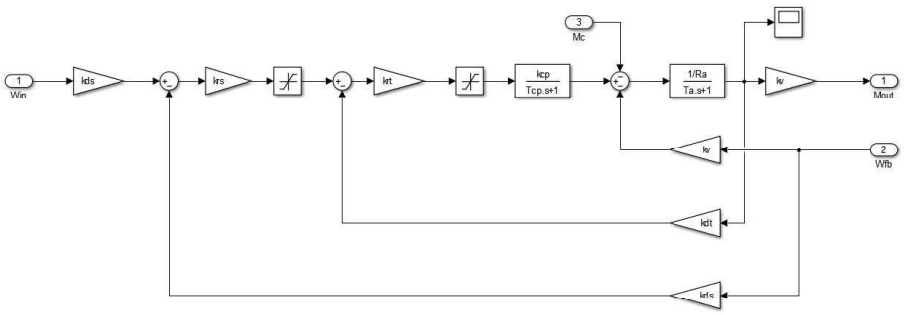

Figure 7.14: DC motor model in Matlab Simulink

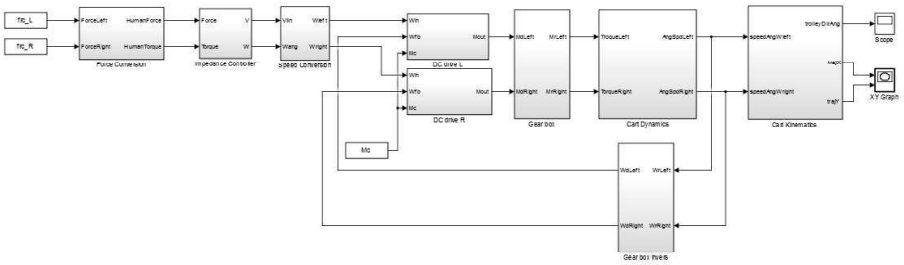

Figure 7.15: Industrial cart model developed in Matlab Simulink

7.7 Impedance control

Impedance control (or admittance control) was developed by N. Hogan [20]. It uses two basic laws of physics such as Newton's second law (see eq. 7.24) and D'Alembert's law (see eq. 7.25). It can be described as a second order dynamic system. Figure 7.16 represents the impedance control scheme using a mass-damper-spring system. In this relationship, impedance is the passive reaction that a robot performs when it is disturbed by external forces. In contrast, admittance control is the active reaction of the robot to such external forces. The "spring coefficient" K defines the force output for a tension or compression of the spring produced by a force F and the "damping coefficient" D is the force output for a velocity input of the displacement x, "mass coefficient" describing the inertia of the system.

$$\sum F_{ext} = ma \tag{7.24}$$

$$\sum F = 0 \tag{7.25}$$

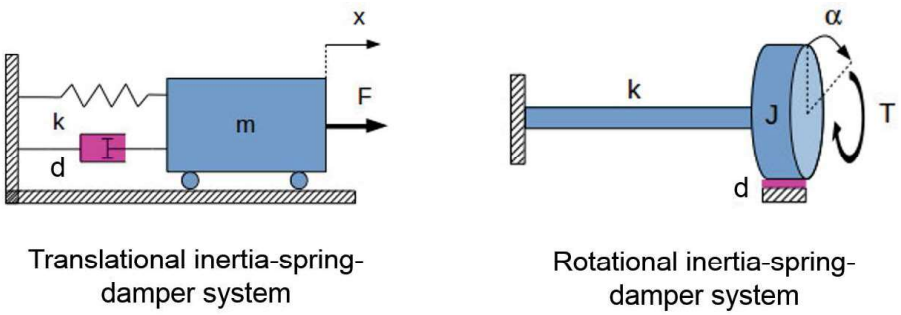

Figure 7.16: Impedance controller representation

Equation 7.26 represent impedance controller for translational motion.

$$M\ddot{x}(t) + D\dot{x}(t) + Kx(t) = -F(t) \tag{7.26}$$

Equation 7.27 represent impedance controller for rotational motion.

$$J\ddot{\alpha}(t) + D\dot{\alpha}(t) + K\alpha(t) = -T(t) \tag{7.27}$$

7.8 Low-level control

In the subsection low-level control the control scheme the of developed powered cart was described. It explains the process of motor setpoints generation based on human-operator intention.

Interaction forces between human-operator and industrial cart are measured by two load cells. Analog values of the forces are converted to the digital format using HX711 24-bit ADCs and sent to the low-level controller (Arduino Mega board)

over SPI. Using equations 7.18 and 7.19 translation force and rotational torque are calculated based on the forces measured from the right and left side of the handle bar. Calculated values are supplied to the corresponding input of transnational and rotational impedance controller. The setpoints for linear and angular velocities of the cart were obtained at the outputs of impedance controllers. Based on the linear and angular velocities the values for angular velocities of the left and right wheels were calculated using equations 7.16 and 7.17. At the last stage the setpoints were processed by the PID controllers of the corresponding wheels. Motors are controlled by the drive unit (MOD-035) using PWM and direction control. Information about actual position and velocity of the wheels is received from the magnetic rotary encoders (AS5040). The parameters of impedance controllers 7.26 and 7.27 could be changed remotely over the serial port of Arduino Mega board.

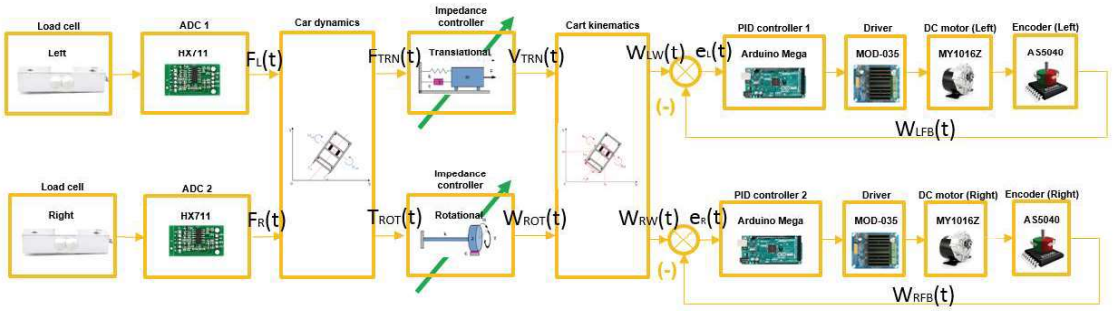

Figure 7.17: Low-level control scheme

Additionally, we had one more micro-controller (Arduino Pro Mini) that was connected to IMU. Using the serial port the IMU controller passed the data through the low-level controller to the high-level controller. Actual information about interaction process was recorded to an SD cart with the time stamp.

8 Human operator study

8.1 Research workflow development

> "That's one small step for man,
> one giant leap for mankind"
>
> Neil Armstrong

In order to find a better solution for human-robot interaction we should understand the nature of human motion, individual motivation and stimulus. This chapter starts with the explanation of the human step nature.

There are two most famous theories about nature of human gait popular in our time. The first theory proposed by Saunders et al. defines six major determinants of gait [33]. It states that the six major determinants are pelvic rotation, pelvic tilt, knee and hip flexion, knee and ankle interaction, and lateral pelvic displacement. The serial observations of irregularities in these determinants provide insight into the individual variation and a dynamic assessment of normal and pathological step.

The second theory of human walking describes the locomotion by using an inverted pendulum model. It states that the stance leg behaves like an inverted pendulum, allowing for economical gait. The advantage of a pendulum is that it conserves mechanical energy and thus requires no mechanical work to produce motion along an arc. Observations of mechanical energy exchange and leg-length change during a single-limb support provide a strong indication of pendulum-like behavior. In the figure 8.1 the process of human walking is shown.

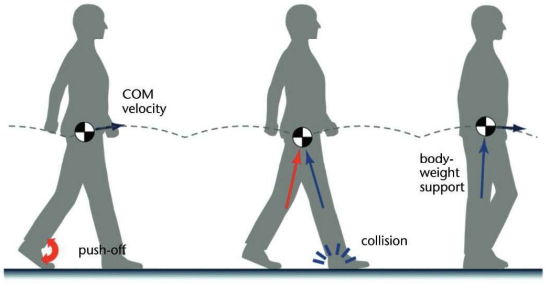

Figure 8.1: Process of the dynamic walking [34]

Another important factor that plays a great role in human - cart interaction is mechanical impedance of the human arm. It describes the motion ability of the

upper limb. This interaction imposes forces on the hand and can also destabilize motion. Alternatively, humans have excellent capabilities to manipulate objects. This means that the central nervous system (CNS) is able to adapt to various task dynamics. For instance, one may have difficulty opening a door for the first time due to an unknown friction. However, after many trials the appropriate force to be exerted will be learned, and one will open the same door without difficulty and even without thinking about it. This situation may be regarded as impedance control [20] which can been described as an effective strategy of the nervous system to deal with kinematic variability due to neuromuscular noise and environmental perturbations.

Biologically, muscle comes with two sections which are thick (myosin) filaments and thin (actin). This part is shown in figure 8.1. Myosin filaments slide against actin which tend to shorten the activated muscle. Neural activation signals are received when the muscle is activated. That signal consists of several spikes. The amount of force it produces depends on the frequency and magnitude of spikes.

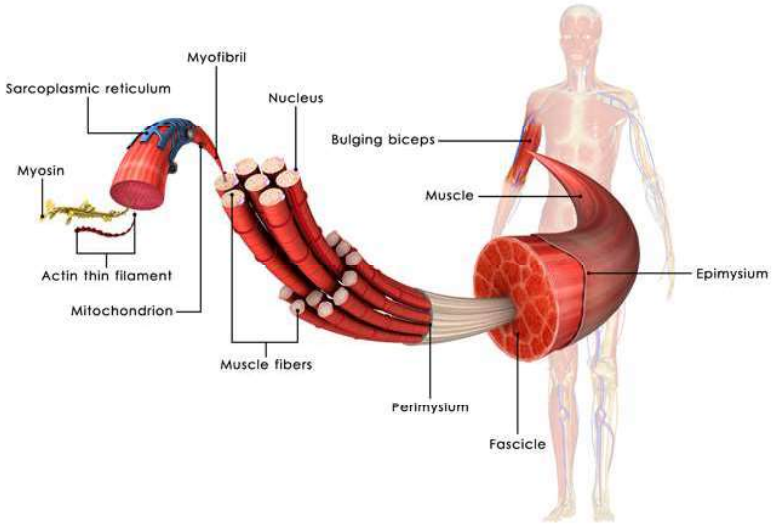

Figure 8.2: Myosin and actin filaments in a muscle [35]

In addition, muscle tension is counted on both length and velocity. Experiment was made by Burdet [36] to measure stiffness (K) and damping (B) for a cat's muscle. As a result, when the length is equal to half of the initial length, the muscle cannot generate the force and the same is right for the velocity. However, the force increases as length or velocity increases. Hence, the impedance of a single muscle changes with the force it generates.

From the aspect of biomechanics systems, the previous study has introduced two types of muscle models which are Maxwell model and Voight model. As it can be seen from the figure 8.3, the Maxwell model consists of a spring in series with a damper while the Voight model has the spring in parallel with a damper. From a prospective of the input it shows that force step input and displacement step input tests from Voight's model is more realistic than Maxwell model [37]. Even though the Voight's model is more realistic, the limitation of both models is that none of

them is capable of modeling the active contractile property of a muscle. After that many researchers came up with a new modeling based on Voight model in order to predict the mechanical impedance of a human's upper limb.

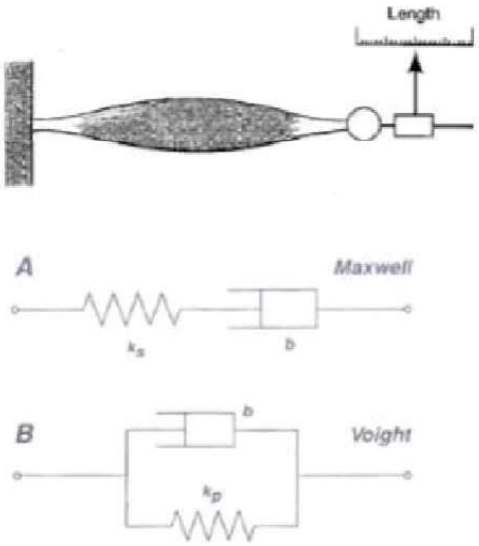

Figure 8.3: Maxwell (A) and Voight (B) muscle models

Mechanical impedance modeling is an important stage in order to determine the quantitative assessment of the system. Each element represents the function of the real human arm. In this section, different modalities will be elaborated. It can be represented in two ways which are the structure model (See figure 8.4) and the mathematical model.

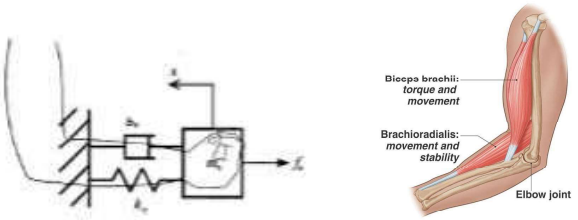

Figure 8.4: Mechanical impedance of the human arm. Structural model [37]. Arm illustration is adopted from [35]

Previous studies had used the MSD systems to a great extent in order to represent a mechanical impedance of human arm [37]-[38]. The mass-spring-damper model is shown in figure 8.4. This is the second order dynamic system where $m_e(t)$, $b_e(t)$, and $k_e(t)$ are the impedance parameters which denote the mass, damping factor, and stiffness of the arm, respectively; and $f_e(t)$ representing the force exerted to the arm. Researchers have done a number of experiments on mechanical impedance of a human arm. Several independent mathematical models are proposed for the representation of the human arm movement. Recently, the MSD model has been

improved to investigate mechanical impedance during the movement of the arm [37]. They have included muscle activation as a dependent parameter [39]. However, this model was developed assuming that the system has simple joints and does not consider complex muscle mechanics and geometry because when dealing with muscle it is not easy as the shape is very irregular. As reported by Speich et al. [40] and Rahman et al. [41] a model with five parameters with additional spring and damper to better approximate the dynamics systems was developed. Then, Wang et al. [42] studied the mechanical impedance during maintained posture and reaching movements in order to analyze human impedance changes depending on the situation. Lagrangian approach is applied to develop the mathematical model of human arm during movement. Tanaka et al.[43] proposed an active-steering control method that uses human hand impedance properties.

8.2 Human Factors, Hazards and Limitations

The industrial cart manipulation is mainly performed by pulling backward and pushing forward with two-hands. Pushing is preferable to pulling for several reasons. Firstly, operator's feet are often "run over" by the cart when pulling. It becomes even more dangerous in case of powered vehicles. If a person pulls while facing in the direction of travel, the arm is stretched behind the body, placing the shoulder and the back in a mechanically awkward position, increasing the risk of injury. Alternatively, pulling while walking backwards is a recipe for an accident, because the person is unable to view the path of travel. Possible poses of the human-operator during manipulation with industrial cart are shown in the figure 8.5.

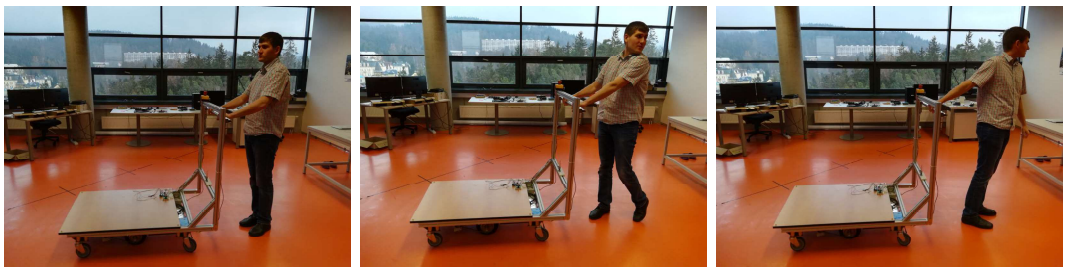

Figure 8.5: Possible poses of the human operator during manipulation with the cart

The research of Lee [44] demonstrates that people can usually exert higher push forces than pull forces. In some situations, pulling may be the only viable means of movement, but such situations should be avoided wherever possible, and minimized when pulling is necessary.

Because of the complex nature of body motion during pushing and pulling, no numerical standard has yet been developed that can be directly applied in the industry.

The amount of force that a worker can develop in case of transnational and rotational motion depends on many factors. The list of factors could be found below:

- body weight and strength
- height of force application
- direction of force application
- distance of force application from the body
- different positions
- posture (bending forward or leaning backward)
- friction coefficient (amount of friction or grip between floors and shoes)
- duration and distance of push or pull

Table 8.1 contains the upper force limits for a variety of pushing and pulling tasks. They indicate the amount of force that a worker should not overcome. It is important to be aware that the forces in the tables are not the same as the weight of objects being pushed and pulled. This difference means that we cannot use these upper force limits as recommendations for weight limits that can be pushed or pulled in the workplace.

The values in Table 8.1 show the upper limits of forces for horizontal pushing and pulling. These limits should not be exceeded in work situations. In fact, it is better and safer if pushing and pulling tasks require lower forces, particularly, where the task requires:

- pushing or pulling an object when the hands must be above the shoulder or below the waist level
- exerting a force for longer than 5 seconds
- exerting a force at an angle not directly in front of the body, e.g., not ”straight on”

Higher forces (up to 675N or about 165 lbf or 75 Kgf) can be developed where a worker can support his body (or feet) against a firm structure.

** Units of force are: Newton (N), kilogram-force (kgf), pound-force (lbf); 10N is about the same as 1 Kgf or 2 lbf. The values in each unit system - Newtons, kilogram force and pound force, respectively - are provided in the table because all are used in the literature and on instruments, depending on the country of origin.

Condition	Force limit(Newtons, lbf, kgf)**	Examples of Activities
A. Standing		
1.Whole body involved	225 N (50 lbf or 23 kgf)	Truck and cart handling. Moving equipment on wheels or casters.
2.Primary arm and shoulder muscles, arms fully extended	110 N (24 lbf or 11 kgf)	Leaning over an obstacle to move an object. Pushing an object at or above shoulder height.
B. Kneeling	188 N (42 lbf or 21 kgf)	Removing or replacing a component from equipment as in maintenance work. Handling in confined work areas such as tunnels or large conduits.
C. Seated	130 N (29 lbf or 13 kgf)	Operating a vertical lever, such as a floor shift on heavy equipment. Moving trays or a product on and off conveyors.

Table 8.1: Recommended Upper Force Limits for Horizontal Pushing and Pulling [45]

8.3 Emotional feedback

The goal of this chapter is to describe the test methods to estimate operator's individual perception in response to the motion of the powered vehicle.

In our study emotional feedback of the human operator is very important and we had to find the way of evaluating subjective human emotions. One way to estimate the operator's feedback is to use the adjective measures in the rating scale method.

This method has been used for measuring how people feel about various stimulus such as sounds, colors or smells. Another application area of this method was ergonomics. It allows to evaluate emotions about the task environment, machine and robot motion.

The method is known as an evaluation tool based on several step-wise measures in which adjective pairs are located at the opposite poles. In the experiment, the person evaluates his emotion according to the adjective pairs. The goal of this measure is to find suitable impedance controller parameters that allow to perform comfort interaction based on subjective feeling.

Therefore, we selected six adjective pairs and rating scale in order to perform human factor analysis. Used rating scale is shown in the figure 8.3. Selected adjective pairs have the following statements:

1. **"comfortable — uncomfortable":** This adjective pair should express the human operator feelings in terms of interaction comfort. It describes how

precisely the dynamics of the powered cart follows the desired motion of the human operator.

2. **"reliable — unreliable":** The adjective pair characterizes trust of the human operator in relation to the powered cart. It means that action of the powered cart fits to the expectations of the human operator.

3. **"controllable — uncontrollable":** We work with the impedance controller for two degrees of freedom. A change or adaptation of the impedance controller parameters affects the ability of the human to control the system. This adjective pair should give the feedback about the controller settings.

4. **"pleasant — unpleasant":** This adjective pair presents the motivation (willingness) of the human operator to use the powered cart.

5. **"satisfactory — unsatisfying":** Human estimation of the interaction task results are characterized by this adjective pair.

6. **"light — heavy":** This adjective pair characterizes physical abilities of the human operator in the load handling.

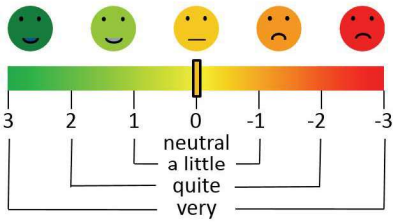

Figure 8.6: Rating scale for the emotional feedback of the human

The evaluation procedure was executed as follows. The operator expressed his feelings by choosing one of seven options in between the opposite poles in each adjective pair according to his/her impression about the controller settings. Given the example of the procedure outcome we could see the test sheet with the following answers:"The controller's setting is neither comfortable, a little reliable, neither controllable, a little pleasant, very light". "Positive" feedback is defined as the mean value located in the left position and "Negative" feedback is defined as the mean value located in the right.

8.4 Physical feedback

"The thesis target is to reach the state where the operator manipulates the heavy loaded cart with minimal physical effort (pleasant and comfortable interaction). Iterative adjustment of controller parameters with continuous force measurement on the operator-cart interface and following recognition of the human-operator intention is expected."

doc. Ing. Petr Tůma, CSc.

This chapter is devoted to the measurement methods of biological features and markers that help to define the health conditions of a person depending on the interaction between the human operator and the industrial cart.

Due to the fact that our goal was to find criteria for human interaction comfort in real-time we used a Borg scale [46] shown in the table 8.2 as a tool for operator's comfort measurement.

Score	Description
6	
7	Very, very light
8	
9	Very light
10	
11	Fairly light
12	
13	Somewhat hard
14	
15	Hard
16	
17	Very hard
18	
19	Very, very hard
20	

Table 8.2: Borg scale (rate per exertion)

The Borg scale [46] was originally developed by the scientist Gunnar Borg who rated the scale from 6 to 20, which was basically built around a heart rate range. This scale correlates with a person's heart rate or how hard they feel they are

working. We use Borg scales in our experiments to evaluate biological markers of the human - cart interaction. The scales are shown in tables 8.2. In addition to Borg scale we used No.1 F4 IP68 Waterproof Smartband for the heart rate measurement. The device is shown in the figure 8.7.

Figure 8.7: No.1 F4 IP68 Waterproof Smartband

Smart band in the figure 8.7 was used to carry out the measurement. The band has the set of functions presented in the figure 8.8. We are interested in such biomarkers as pulse, blood pressure, saturation and the number of steps made. The standard use of the band involves the connection to the mobile phone to read the statistical data through the bluetooth interface. The statistics it receives can be visualized in a certain application. The idea was to replace the mobile phone application backend with a custom program, so that it could receive the information on the condition of biological markers and forward this information to the high-level controller.

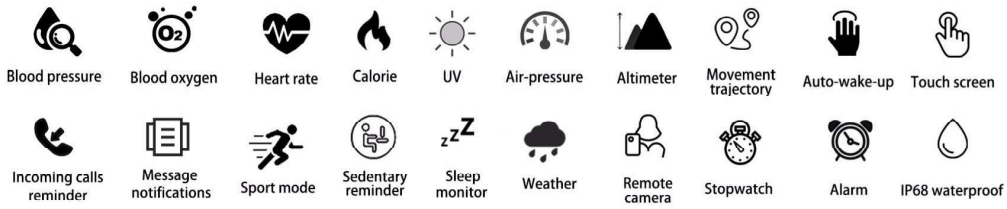

Figure 8.8: List of features

As a higher level controller a microcomputer Raspberry Pi, version 4 was used. An application called "GATTacker" was used as a tool to perform the task in order to intercept bluetooth packages and carry out the data analysis. As a result, package structure was identified. This information allowed me to create a Python script which could connect to the smart band from the high-level controller over bluetooth.

The script was able to read the pulse, blood pressure and blood oxygen saturation in real time. The tool chain described above allowed me to follow the biomarkers of a human operator during the interaction process with a powered industrial cart. To measure the pulse, blood pressure, and saturation the band used the sensor based on the photoplethysmogram principle.

A photoplethysmogram (PPG) is an optically obtained plethysmogram that can be used to detect blood volume changes in the microvascular bed of tissue. A PPG is often obtained by using a pulse oximeter which illuminates the skin and measures changes in light absorption.[47] A conventional pulse oximeter monitors the perfusion of blood to the dermis and subcutaneous tissue of the skin.

With each cardiac cycle the heart pumps blood to the periphery. Even though this pressure pulse is somewhat damped by the time it reaches the skin, it is enough to distend the arteries and arterioles in the subcutaneous tissue. If the pulse oximeter is attached without compressing the skin, a pressure pulse can also be seen from the venous plexus, as a small secondary peak.

The change in volume caused by the pressure pulse is detected by illuminating the skin with the light from a light-emitting diode (LED) and then measuring the amount of light either transmitted or reflected to a photodiode. [48] Each cardiac cycle appears as a peak, as seen in the figure. Because blood flow to the skin can be modulated by multiple other physiological systems, the PPG can also be used to monitor breathing, hypovolemia, and other circulatory conditions. [49] Additionally, the shape of the PPG waveform differs from subject to subject, and varies with the location and manner in which the pulse oximeter is attached.

Smart band uses an accelerometer MC3413 to detect the number of steps. The parameters of the sensors are demonstrated in the data sheet [50].

In order to design the adaptive interaction controller we have to find a dependency between the emotional feedback of the human operator and a measurable physical equivalent. In our case we use the following physical measures per sample time period $T_{sample} = 60s$:

1. Mean and standard deviation of absolute interaction force value - $mean(|F_{interaction}|)$ and $SD(|F_{interaction}|)$
2. Mean and standard deviation of absolute interaction torque value - $mean(|\tau_{interaction}|)$ and $SD(|\tau_{interaction}|)$
3. Mean and standard deviation of absolute linear speed of the cart - $mean(|v_{cart}|)$ and $SD(|v_{cart}|)$
4. Mean and standard deviation of absolute angular speed of the cart - $mean(|\omega_{cart}|)$ and $SD(|\omega_{cart}|)$
5. Heart rate
6. Blood pressure
7. Oxygen saturation

9 Human-cart interaction

9.1 Procedure description

In this chapter the process of human – industrial power assisted cart interaction is described. In the process of moving goods by a human operator with the help of the powered cart on the surface, we have the interaction between cart, human and the environment. Figure 9.1 depicts the diagram of interconnections in human – industrial cart interaction.

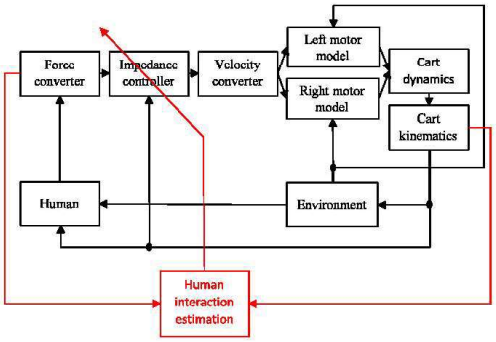

Figure 9.1: Interconnections in human – industrial cart interaction

The task of moving cargo can be divided into five stages. Task scheme is shown in the figure 9.2. The first stage begins with the person's intention to carry out the act of moving goods using an industrial cart. The person has knowledge about the start and end points of the trajectory, the state of the environment. The operator can estimate the force needed to be applied in order to move the load and the powered cart from the start to the end points of the trajectory. He also may or may not have experience of interaction with a powered industrial cart.

The second stage is the initial impact. This stage starts the moment human hands touch a mobile cart. The cart is at rest at the point P_0, which is taken as a point of origin. We take the time of the first touch as the task starting time in the system of a mobile cart. From the point of view of the cart, the force applied by the human is a stochastic variable, since the cart has no information about the real world (knowledge about the weight of the load, the type of surface, the position in space and the desires of a man). Operator's force is divided into rotational and translational components. Then, the desired dynamics of the interaction is set

by relevant impedance controllers. On the output of the impedance controller we obtain the desired linear and angular velocity. Obtained values become a reference setpoints for the differential drive system. The motors run in order to reach the reference value and support the motion.

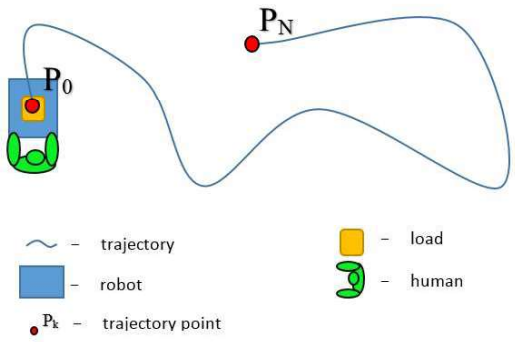

Figure 9.2: Moving cargo task

The third stage – motion task. During this phase the process is about the accumulation of interaction experience. Human-operator and cart find out the information about the response of the system (the change in the interaction force, acceleration, speed, distance, heart rate, oxygen saturation and blood pressure). In case of a mismatch of the expected response of the system obtained by a person during the first phase with the reaction of the real system, the operator estimates the correction of the applied force according to the new data and adapts to them.

The fourth phase is a positioning task. The man performs the application of forces to the cart in order to stop the motion and reach the desired position. The fifth stage is the end of the interaction. This stage comes as soon as the person ceases to interact with the industrial cart. The point P_N is the end of the interaction and the endpoint of the path. The operator achieved his goal. The cart can perform analysis of the completed tasks.

In the phase of the positioning task the distances to the target and the actual traversed path are not equal. Over-reaching the target is influenced by the support of a power assistance system. In this case, the operator must perform additional manipulations to return to the target point. If power assistance is insufficient and cannot go beyond the total value of friction forces that resist to motion, then the distance to the target and the actual traversed path will be equal, but the operator spends additional effort to overcome the friction forces.

9.2 Raw data analysis and feature detection

> "Measurement is the first step that leads to control and eventually to improvement. If you can't measure something, you can't understand it. If you can't understand it, you can't control it. If you can't control it, you can't improve it."
>
> H. James Harrington

Figure 9.3 shows force sensors information when the human assistance ratio is bigger than the desired value and the mobile cart moves faster than the human-operator wants it to move. Periodic oscillations around -40/-50N in the middle of the curve demonstrate the human steps during the motion. Using this information we can estimate the motion rate, human step time, number of steps, step distance. Oscillations around zero in the beginning and in the end of curve characterize the noise caused by the powered cart motion.

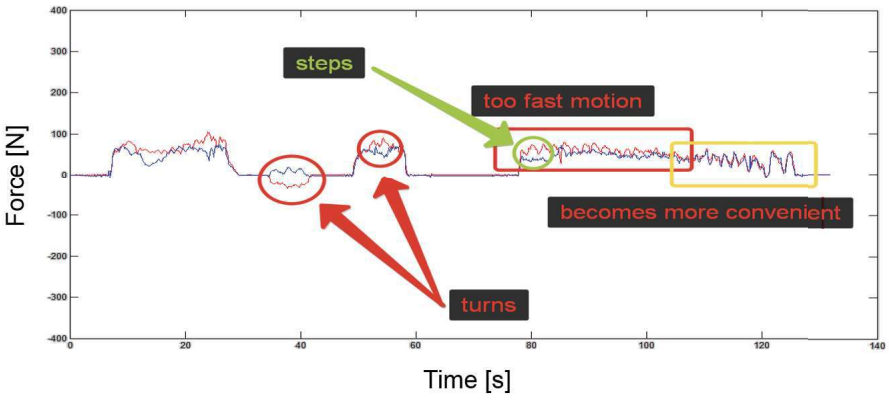

Figure 9.3: Raw data sample from pHRI handlebar

According to the measures defined in the chapter 8.4 we developed a few feature detection techniques to estimate them. In our application we detect human gait by processing of the filtered signal that comes form tensiometers located at the handle bar.

At a later stage, the peak detection and error cancellation algorithm was applied to the signal. At the pipe output we received the information about the amount of steps per task, step time (mean+std), step length (mean+std). The example of the processed data is shown in the figure 9.4.

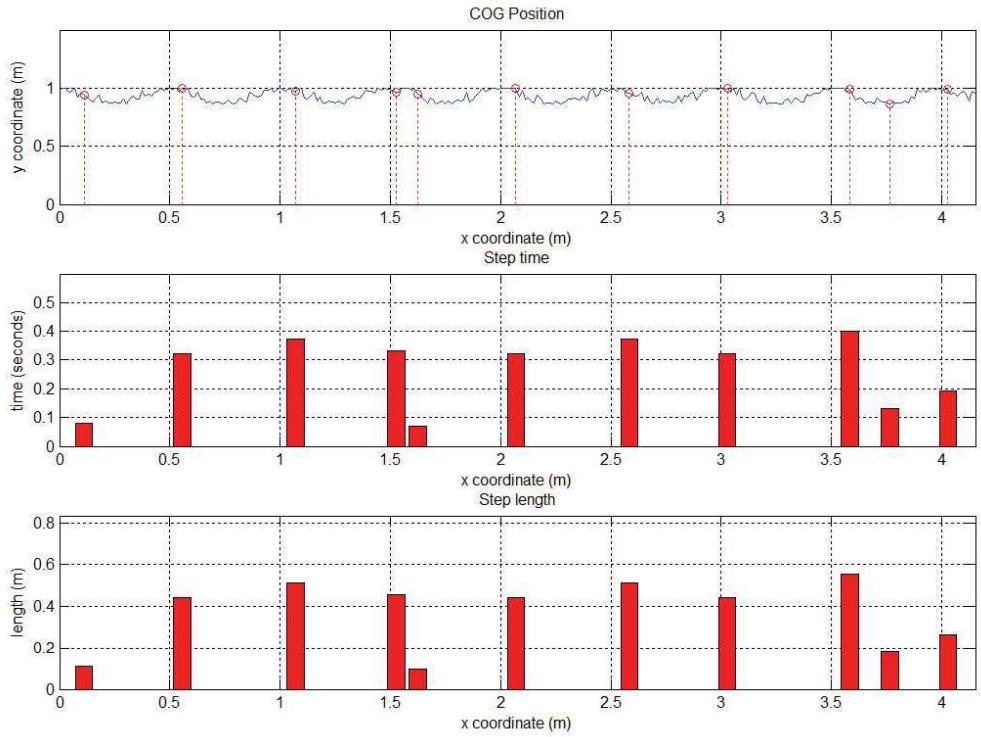

Figure 9.4: Human gait feature

9.3 Effect of the impedance control

We conducted several experiments with different settings of the controller. In each experiment operator with powered cart cyclically performed a front and back motion. A gradual increase of the virtual inertia (mass) is shown in figure 9.5. As we can see, the operator force required for the cargo transportation is reducing (charts from black to green). However, upon further reduction of the ratio (red graph), there was a situation in which the momentum generated by the support system created uncomfortable interaction conditions and operator had to make significant efforts to implement the desired motion.

The graph shows the standard derivative of absolute value of interaction force using various settings of the impedance controller. We change the values of the impedance controller, i.e. its mass component (virtual mass). The time lapse of the sample is 60 seconds, the number of measurements was 120, which means we can generate 3 data samples.

In these cases when the mass component of the impedance control provides minimum or maximal value, the operator has to put a lot of effort to move the loaded trolley. If we consider both the standard derivative and the mean value it is noticeable that it requires a lot of effort from an operator. The reason for that was described in the figure 9.5 - the operator applies force which is transferred by the impedance controller into setpoints for the differential drive system. In case of

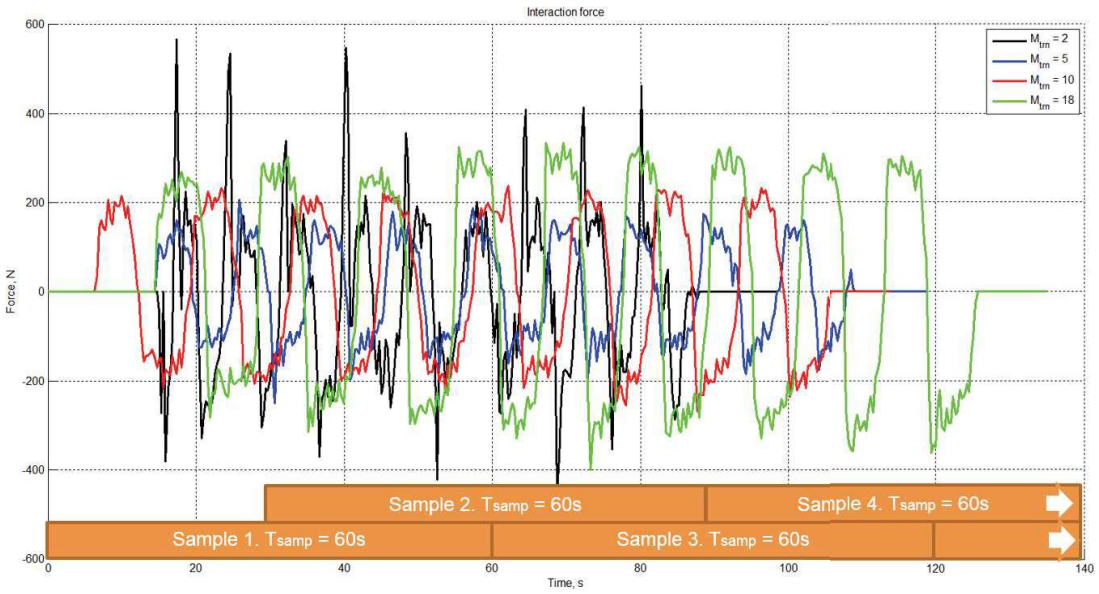

Figure 9.5: Change of interaction force with different settings of the impedance controller [28]

small mass component, the task for the motor appears to be large. The engine works with greater speed which means that the operator has to stop the trolley. On the contrary, if the operator stops the trolley abruptly, the engine will get a large task and start moving the trolley backwards, again, the operator has to stop it not to be run over. In case of large mass component, vice versa, the initial force is great, but the task for the engine is small, which means that the trolley does not help the operator to an extent he desires. None of these modes of mass component works well.

The comfort of the cart operator largely depends on the impedance controller settings. The cart is usually pulled or pushed with two hands. However, if the load is small (light), the cart could be handled with one hand or even with fingers. Each human hand has its inertial, damping and stiffness component (property) as described in the section 8.1.

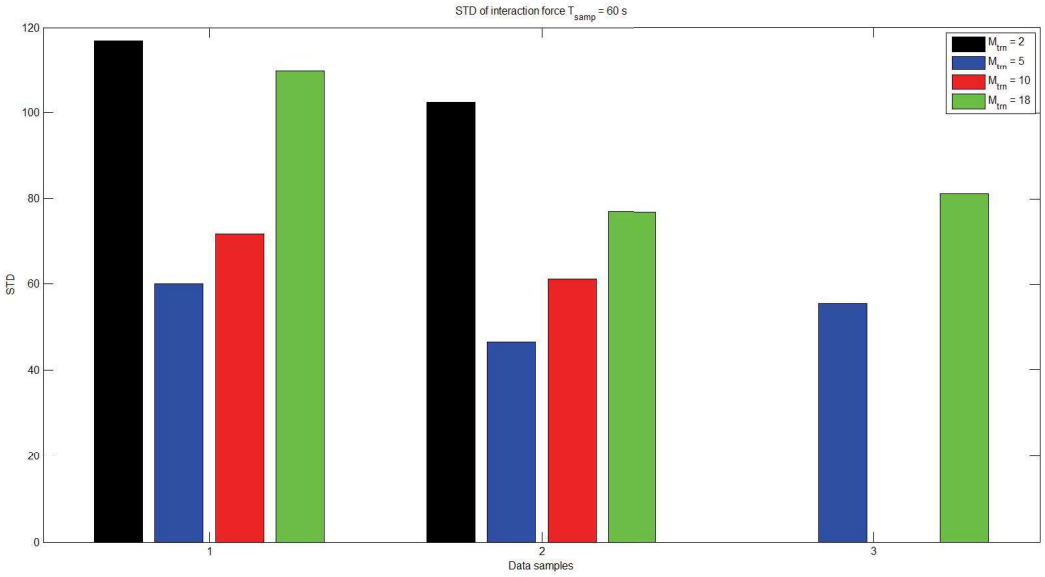

Figure 9.6: Change of interaction force with different settings of the impedance controller [28]

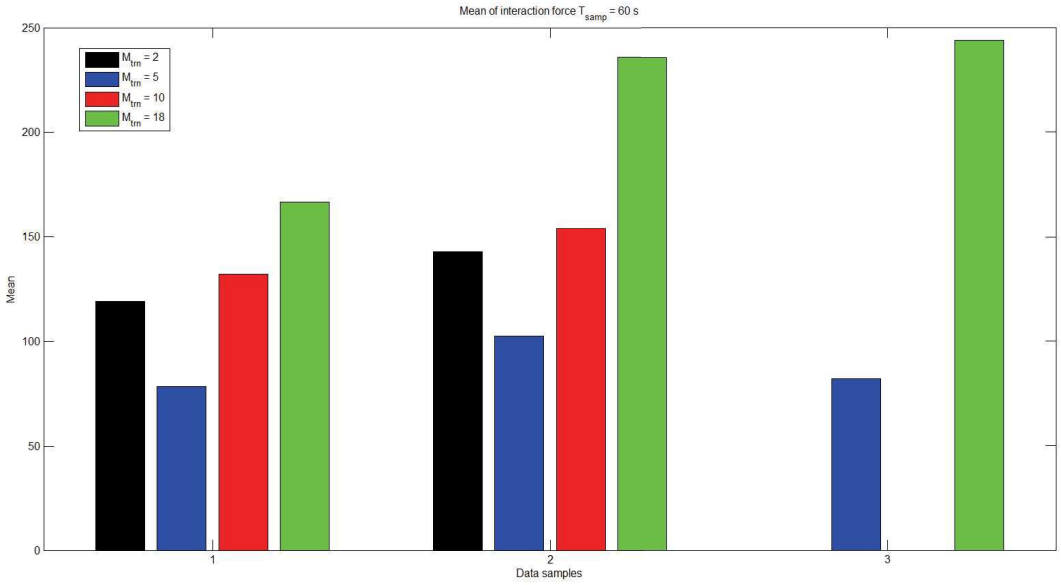

Figure 9.7: Change of interaction force with different settings of the impedance controller [28]

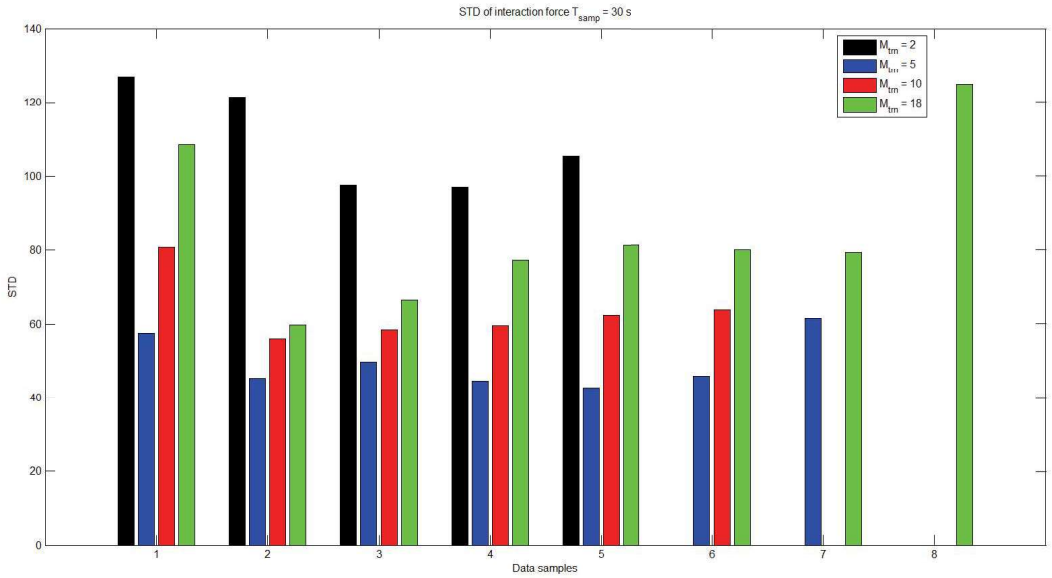

Figure 9.8: Change of interaction force with different settings of the impedance controller [28]

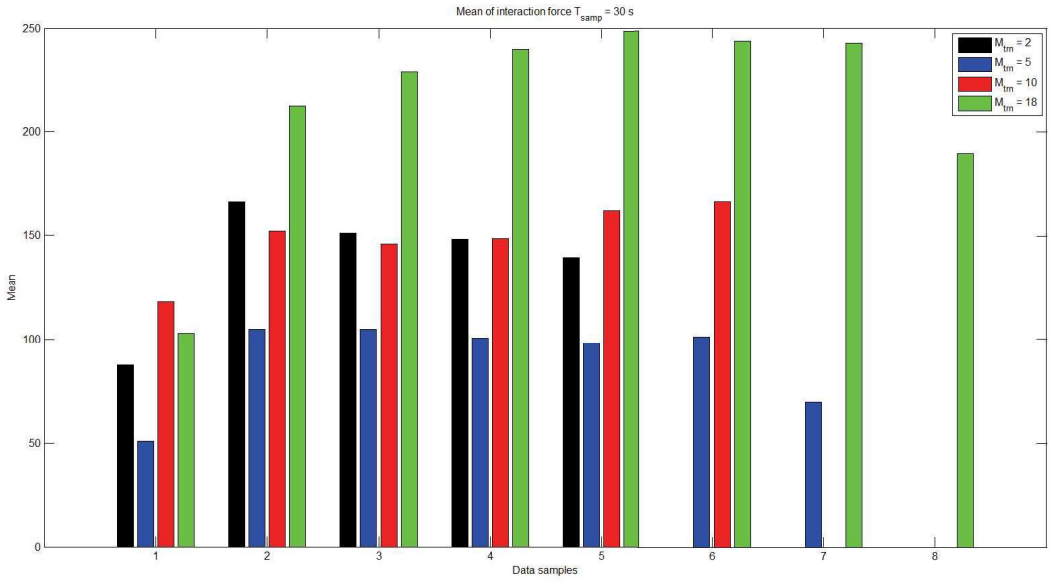

Figure 9.9: Change of interaction force with different settings of the impedance controller [28]

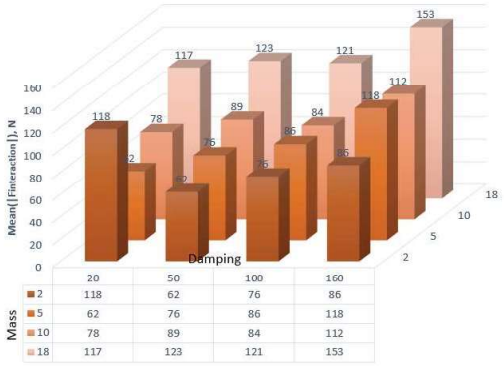

Figure 9.10: Mean value of absolute interaction force for different settings of impedance controller. Sample 1. $T_{samp} = 60s$.

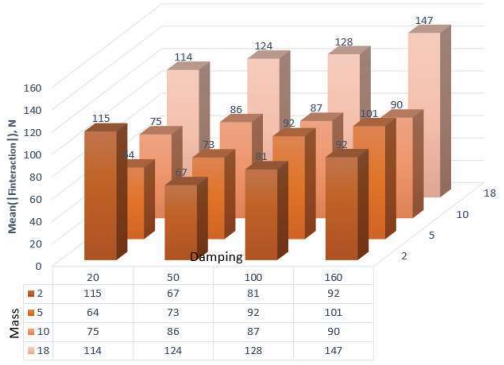

Figure 9.11: Mean value of absolute interaction force for different settings of impedance controller. Sample 2. $T_{samp} = 60s$.

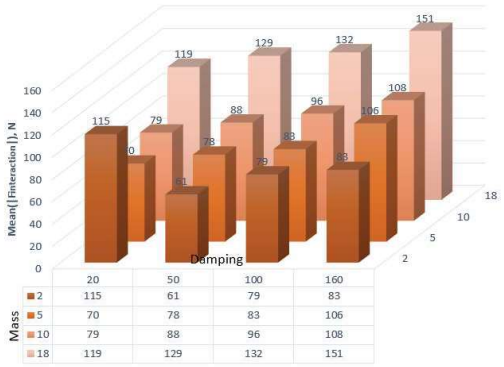

Figure 9.12: Mean value of absolute interaction force for different settings of impedance controller. Sample 3. $T_{samp} = 60s$.

9.4 Experiment design

This chapter highlights the experiments carried out using the mobile platform during the research project. In this chapter we would like to describe the set of performed experiments to measure the interaction parameters between the human operator and industrial cart. The goal of the experiments is to find the relationship between the subjective operator's estimation of the interaction process and measured physical quantities.

The experiments were executed in the laboratories of the Institute for Nanomaterials, Advanced Technologies and Innovation. The coefficients of static and kinetic friction equal to 1 and 0.7 respectively, because of the fact that the floor material is concrete. The laboratory area allowed to simulate material handling tasks related to warehouses, production area, offices and supermarkets.

The subject pool consisted of 5 humans (three males and two females). Two male operators out of the pool had experience in driving powered vehicles. The other experiment members operated the vehicle for the first time. Experienced and inexperienced operators were needed to cover the variance of operator expectations from their interaction with the powered cart. Basic anthropometric data for the operators is presented in the table 9.1.

Figure 9.13: Operator's motion task

N	Parameter	Mean ± Standard Deviation
1	Age	28 ± 5.2 [a]
2	Weight	80 ± 20.8 [kg]
3	Height	180 ± 10.5 [cm]
4	Legs Length	90 ± 12.5 [cm]

Table 9.1: Operators parameters

The participants had to push and pull a six wheeled powered cart on given trajectories. In the experiment five types of trajectories 9.14 were used such as linear path with the length of 5 [m] in order to estimate the effect of the translational impedance controller parameters on human feelings during the transnational motion, circular path was used to verify the effect of the rotational impedance controller [51], eight-like trajectory to test the joint work of the controllers and trajectory with the complex shape similar to a real production scenario as shown in the figure 9.16. At

the end human operators could evaluate their feelings of the collaboration on the free-run trajectory.

Figure 9.14: Trajectory setups

In order to simulate the different load a set of barrels was used. The set consists of five 30 [l], two 50 [l] barrels and two metal pipes that weighted of 50 [kg] each. All the barrels were filled with water. Their weight was measured before the experiment. As a result it was possible to change the cart load in a range $m_{load} \in [0; 340][kg]$. The load set is shown in the figure 9.15.

Figure 9.15: Load variation

In our study we performed the measurement of emotional feedback. Methods from the section 8.3 were used to estimate the individual feelings of a particular operator. The subjective impressions were documented with questionnaires and processed. In addition to emotional feedback, the physical measures were performed. Readings of the interaction process values were recorded (respectively translational and rotational components of position, speed, acceleration from wheel encoders; orientation, angular velocities and linear accelerations form IMU unit, motors currents form motors current sensors, interaction torque and force form tensiometers).

In order to implement power assistance for the industrial cart the low-level control system form section 7.8 was programmed into the micro-controller. Developed system allows to study the effect of different impedance controller settings on the interaction process. Parameter's values for translational and rotational impedance

controller settings were combined in a table 9.2. Based on the parameter's values the experimental test sets were generated. We evaluate the effects of the controller' settings on the operator's comfort. The results of the experiments were collected in the chapter 10.

Translational Impedance Controller

M	Dtrn	Ktrn
2	20	20
5	50	60
10	100	80
18	160	

Rotational Impedance Controller

J	Drot	Krot
1	10	10
4	20	40
8	50	80
18	160	

Table 9.2: Tested impedance controller settings

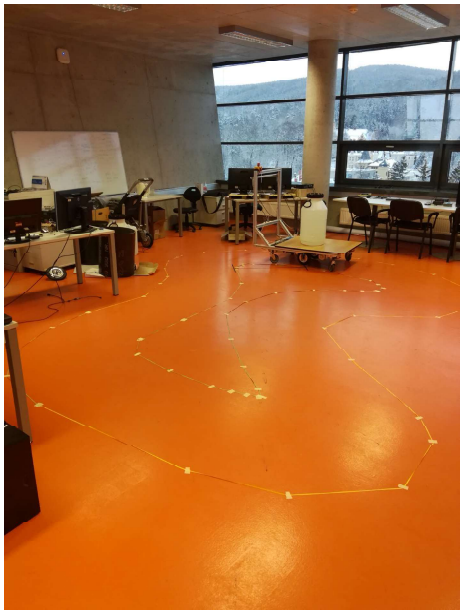

Figure 9.16: Predefined track. Setup for $m_{load+cart} = 103[kg]$

Figure 9.17: Setup for $m_{load+cart} = 163.4[kg]$

Figure 9.18: Setup for $m_{load+cart} = 218.3[kg]$

10 Regression analysis

Regression analysis is a reliable method of identifying which variables have impact on a topic of interest. The process of performing a regression allows us to confidently determine which factors matter the most, which factors can be ignored, and how these factors influence each other.

In order to understand regression analysis fully, it is essential to comprehend the following terms:

1. **Dependent Variable:** This is the main factor that we would like to understand or predict

2. **Independent Variables:** These are the factors that we have an impact on your dependent variable according to our hypotheses.

In this chapter we will perform the regression analysis of data sets that were obtained in the experiments such as human-operator feedback and physical measures. The data collected from the feedback surveys allows us to measure the human-operator feeling, that our operators associate with different settings of impedance control. We could also identify what variables influence those feelings.

In the first analysis we will study the effect of impedance controller parameters on comfort. We select operator comfort as dependent variable and parameters of impedance controller as independent variables. The analysis results are shown in the table 10.1.

If we look at the R-Square value we could conclude that for 48 observations 36% of change in the operator comfort was caused by impedance controller parameters. Significance value F is smaller than 0.05, so regression is strong. When we check the coefficients values we can see that we have a negative relationship between human comfort and the values of mass and dumping coefficients. In simple words, the increase of mass and dumping coefficient leads to the decrease of operator comfort for the analyzed data set. If we look at the P-value for the coefficients we could say that P-values for mass and damping coefficients are lower than 0.05 that means the regression is strong, however the P-value of spring coefficient is much higher than 0.05 and as a result it does not affect operator's comfort.

In the next step we will study the effect of independent variables such as the mean value of absolute interaction force and its standard deviation as well as mean value and standard deviation of absolute linear velocity of the cart. Results are collected in the 10.2. When we analyze R-Square for 48 observations, 78% of change

Regression Statistics	
Multiple R	0.632
R Square	0.400
Adjusted R Square	0.359
Standard Error	1.734
Observations	48

ANOVA

	df	SS	MS	F	Significance F
Regression	3	88.090	29.363	9.771	4.65E-05
Residual	44	132.222	3.005		
Total	47	220.313			

	Coefficients	Standard Error	t Stat	P-value	Lower 95%	Upper 95%
Intercept	2.726	0.786	3.467	0.001	1.141	4.311
Mass	-0.172	0.04	-4.332	8.42E-05	-0.252	-0.092
Damping	-0.012	0.004	-3.248	0.002	-0.019	-0.004
Stiffness	4.17E-18	0.006	7E-16	1	-0.012	0.012

Table 10.1: Regression analysis for comfort of the operator 1 using impedance controller coefficients

in the operator comfort caused by change in interaction force and linear velocity of the cart. Significance value F is smaller than 0.05, so regression is strong.

Regression Statistics	
Multiple R	0.882
R Square	0.778
Adjusted R Square	0.757
Standard Error	1.067
Observations	48

ANOVA

	df	SS	MS	F	Significance F
Regression	4	171.386	42.847	37.656	1.58E-13
Residual	43	48.926	1.138		
Total	47	220.313			

	Coefficients	Standard Error	t Stat	P-value	Lower 95%	Upper 95%
Intercept	4.272	0.979	4.363	7.91E-05	2.297	6.247
Mean Abs F	-0.031	0.011	-2.935	5.34E-05	-0.052	-0.01
Std Abs F	-0.014	0.005	-2.73	9.13E-03	-0.025	-0.004
Mean abs V	5.666	1.9	2.982	0.005	1.834	9.499
Std abs V	-5.419	1.497	-3.619	0.001	-8.438	-2.4

Table 10.2: Regression analysis for operator 1 comfort using mean value and standard deviation of interaction force and cart velocity

We can see that the mean and standard deviation of absolute interaction force and cart velocity has a significant effect on human-operator comfort, because the P-value of each parameter is higher than 0.05. We apply regression analysis to

data sets of all the operators and as a result we could confirm that the interaction force and cart velocity have a significant effect on human-operator comfort, however for different operators comfort state is reached with different impedance controller setting.

In the third step we study the relationship between operator comfort and biological markers such as pulse, blood pressure, oxygen saturation. The results were combined in the table 10.3. After analysis of R-Square for 48 observations it could be concluded that 81% of change in the operator's comfort is caused by biological markers. Regression is strong, because the significance value F is smaller than 0.05. It could be observed that the heart rate and comfort of the human-operator have a negative relationship. It means that the human-operator heart rate is getting lower when the comfort zone is reached as well as the heart rate is increasing when a lot of effort is needed to overcome the friction force or return the cart to a desired position if the target was over-reached. Oxygen blood saturation and Borg scale estimations have positive relation to the operator's comfort. If we look at the P-value for the coefficients we could say that only P-value of oxygen blood saturation is lower than 0.05 that means the regression is strong only for this parameter.

Regression Statistics	
Multiple R	0.9
R Square	0.81
Adjusted R Square	0.797
Standard Error	0.976
Observations	48

ANOVA

	df	*SS*	*MS*	*F*	*Significance F*
Regression	3	178.378	59.46	62.39	6.87E-16
Residual	44	41.934	0.953		
Total	47	220.313			

	Coefficients	*Standard Error*	*t Stat*	*P-value*	*Lower 95%*	*Upper 95%*
Intercept	-123.766	48.772	-2.536	0.015	-222.061	-25.474
HR	-0.072	0.048	-1.49	0.143	-0.17	0.025
SPO2	1.3	0.482	2.696	0.01	0.329	2.273
Borg Scale	0.25	0.387	0.647	0.521	-0.529	1.03

Table 10.3: Regression analysis for operator 1 comfort using biological markers

The results of the regression analysis of the data set that includes all the participants are shown in the tables 10.4 - 10.6. The data set of all participants includes 240 observations. In the table 10.4 we analyze the effect of impedance controller parameter's change on comfort of different operators. The R-Square for 240 observations equals to 0.332. It means that only 33% of change in the operator comfort caused by the change of controller parameters. The regression is strong, because significance value F is smaller than 0.05. The relationship between human comfort and the values of mass and dumping coefficients is negative. The P-value for the coefficients shows that the regression is strong, however the P-value of spring coefficient is much higher than 0.05 and as a result it does not affect operator's comfort.

Regression Statistics	
Multiple R	0.576
R Square	0.332
Adjusted R Square	0.324
Standard Error	1.727
Observations	240

ANOVA

	df	SS	MS	F	Significance F
Regression	3	350.433	116.811	39.146	1.43E-20
Residual	236	704.217	2.98		
Total	239	1054.65			

	Coefficients	Standard Error	t Stat	P-value	Lower 95%	Upper 95%
Intercept	2.386	0.35	6.808	8.12E-11	1.695	3.075
Mass	-0.147	0.018	-8.258	1.06E-14	-0.181	-0.112
Damping	-0.011	0.002	-7.017	2.39E-11	-0.014	-0.008
Stiffness	-4.06E-18	0.003	-1.49E-15	1	-0.005	0.005

Table 10.4: Regression analysis for comfort of all the operators using impedance controller coefficients

The result of the regression analysis for comfort of all the operators using the mean value and standard deviation of interaction force and cart velocity was collected in the table 10.5. For complete data set of all participants the 79% of change in the human comfort is caused by the mean value and standard deviation of measured interaction force and cart velocity. Significance of the F value is less that 0.05 demonstrates strong regression. The P-value of all the coefficients less than 0.05 shows that all the physical measures have an effect on the operator's comfort.

Regression Statistics	
Multiple R	0.87
R Square	0.757
Adjusted R Square	0.753
Standard Error	1.044
Observations	240

ANOVA

	df	SS	MS	F	Significance F
Regression	4	798.702	199.675	183.333	4.98E-71
Residual	235	255.948	1.089		
Total	239	1054.65			

	Coefficients	Standard Error	t Stat	P-value	Lower 95%	Upper 95%
Intercept	3.909	0.422	9.257	1.36E-17	3.077	4.741
Mean Abs F	-0.033	0.005	-6.945	3.67E-11	-0.042	-0.023
Std Abs F	-0.011	0.002	-4.888	1.88E-06	-0.016	-0.007
Mean Abs V	6.555	0.874	7.502	1.28E-12	4.833	8.276
Std Abs V	-5.79	0.696	-8.313	7.51E-15	-7.162	-4.418

Table 10.5: Regression analysis for comfort of all the operators using mean value and standard deviation of interaction force and cart velocity

Table 10.6 shows the effect of biological markers on operator's comfort. The result of the regression analysis demonstrates that 81% of change in the human

comfort is caused by biological markers. Significance of the F value is less than 0.05 demonstrates a strong regression. The P-values of the heart rate and oxygen blood saturation coefficients are less than 0.05. It shows that biological markers indicates the operator's comfort.

Regression Statistics	
Multiple R	0.902
R Square	0.814
Adjusted R Square	0.811
Standard Error	0.913
Observations	240

ANOVA

	df	*SS*	*MS*	*F*	*Significance F*
Regression	3	858.052	286.017	343.341	9.14E-86
Residual	236	196.598	0.833		
Total	239	1054.65			

	Coefficients	*Standard Error*	*t Stat*	*P-value*	*Lower 95%*	*Upper 95%*
Intercept	-134.406	20.212	-6.65	2.02E-10	-174.225	-94.586
HR	-0.067	0.02	-3.278	0.001	-0.107	-0.027
SPO2	1.405	0.2	7.029	2.22E-11	1.011	1.799
Borg Scale	0.235	0.163	1.446	0.149	-0.085	0.556

Table 10.6: Regression analysis for comfort of all the operators using biological markers

When we evaluate participants separately the output of the regression analysis was similar to the results demonstrated in tables 10.1 - 10.3. However, the analysis of data for all operators shows a different result. As it could be observed form the table 10.4 the R-Square value is significantly reduced in comparison to individual approach. It means the impedance controller settings that could be evaluated as comfortable are different from one operator to another. In fact, dependency between the comfort, mean and standard values of interaction force and cart velocity as well as biological markers remains the same. It allows us to conclude that the mean value and standard deviation of interaction force and cart velocity as well as heart rate and oxygen blood saturation could be used as a sufficient reference for generation of the rewards for the reinforcement learning algorithm.

11 Q-Learning for human-cart interaction

"When you first start off trying to solve a problem, the first solutions you come up with are very complex, and most people stop there. But if you keep going, and live with the problem and peel more layers of the onion off, you can often times arrive at some very elegant and simple solutions."

Steve Jobs

In this chapter the control algorithm that was developed for robust and safe physical interaction between the human and industrial cart will be described. As it was demonstrated in chapter 3 the impedance control is an essential component of the solution. It could be used as a part of representation for the human-operator dynamics as well as it helps us to control supporting effort of the mobile platform side during collaboration. Possible scenario is shown in the figure 11.1.

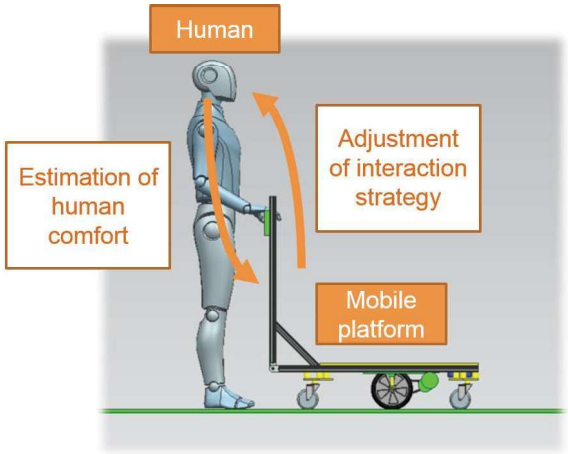

Figure 11.1: Physical collaboration scenario

While performing the task the human operator learns based on his estimations and feelings. As a result, he adapts his impedance according to the required effort for the task. As it was shown in numerous force field tasks, humans combine

two strategies to adapt their impedance to perturbations, thereby minimizing position error and energy consumption: 1) if perturbations are unpredictable, subjects increase their impedance through co-interaction; and 2) if perturbations are predictable, subjects learn a feed-forward command to offset the perturbation [52].

On the other hand, the mobile platform adjusts the interaction strategy by changing the impedance parameters. The change occurs according to the correlation between detected features and human feelings that was found in the chapter 10.

A Markov decision process or an MDP consists of

- S, a set of states of the world.
- A, a set of actions.
- $P : S \times S \times A \rightarrow [0, 1]$, which specifies the dynamics. This is written as $P(s'|s, a)$, where $\forall s \in S$; $\forall a \in A$; $\sum_{s' \in S} P(s'|s, a) = 1$. In particular, $P(s'|s, a)$ specifies the probability of transitioning to state s' given that the agent is in a state s and does action a.
- $R : S \times A \times S \rightarrow R$, where $R(s, a, s')$ gives the expected immediate reward from doing action a and transitioning to a state s' from the state s.

Both the dynamics and the rewards can be stochastic; there can be some randomness in the resulting state and reward, which is modeled by having a distribution over the resulting state and by R giving the expected reward. The outcomes are stochastic when they depend on random variables that are not modeled in the MDP.

A finite part of a Markov decision process can be depicted using a decision network as in Figure 11.2.

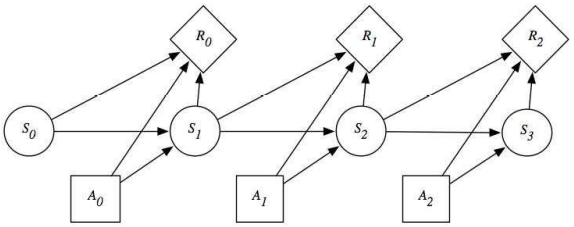

Figure 11.2: Decision network representing a finite part of an MDP [53]

In order to include human feelings in the control system we implemented a reinforcement learning algorithm. The book "Reinforcement Learning: An Introduction" [54] is giving the following definition to the reinforcement learning:

"Reinforcement Learning is an area of Machine Learning that can be considered both a set of problems and solution methods to these problems. It is concerned with finding the best possible behaviour strategy for an agent interacting with an environment. The underlying idea is that similarly to how humans and other animals learn by trial-and-error, so should also software agents be able to learn."

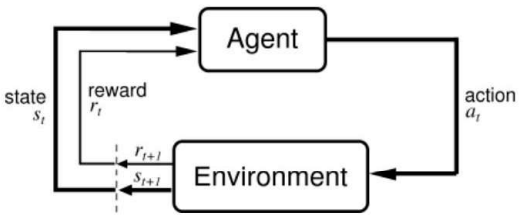

Figure 11.3: Reinforcement learning flow diagram [54]

Reinforcement Learning was originally inspired by behavioural psychology. Similarly to how humans are taught that some actions are good and others are bad by either reward or punishment, this class of algorithms reinforces good actions while discouraging bad. For example, teaching a dog to catch the ball by rewarding it with a bone if successful as shown in the figure 11.4. This trial-and-error approach to learning is simulated by giving a numerical reward as a feedback on the performance of an algorithm. Thus, based on the result signal, a learning algorithm can evaluate and update its parameters based on how good or bad a set of actions were.

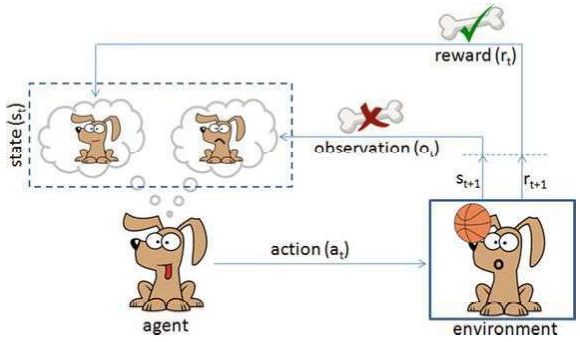

Figure 11.4: Natural way of RL [55]

Reinforcement learning algorithms are built of the following main components [56]:

- `State.` Set S of states the agent and environment can be in.
- `Actions.` Set A of actions the agent can invoke. This set can be restricted depending on the current state.
- `Reward.` R is a function that provides numerical rewards for state transitions. It is used to estimate the quality of action a_t in state s_t based on the state change it causes.
- `State Variables.` The value map memorizes what outcomes an agent expects for given states
- `Policy.` A policy is a structure that maps states to actions. Roughly speaking, it defines what action to take in a specific state.

- `Model (Optional).` A model of the environment and agent predicts the new state s' when action a is invoked in states. The model can be probabilistic or unavailable.

The first task when designing Q-Learning system is to define the environment. The environment consists of states, actions and rewards. The agent uses states and rewards as inputs and generates actions as outputs.

11.1 States

The number of possible states is finite. The agent could be in one fixed number of possible situations. In our case we can think about each possible setting of impedance controllers as a state. The agent could be located at one state at a time. It means only one set of impedance controller settings could be selected in one step and evaluated in one step. Each component of the impedance controller could switch in between four states. According to the selected parameters of the impedance controllers shown in the table 9.2 with neglected parameters of K_{trn} and K_{rot} the set of 256 system states was generated.

States[256] = generate

M	Dtrn	J	Drot
2	20	1	10
5	50	4	20
10	100	8	50
18	160	18	160

Figure 11.5: Set of states

11.2 Actions

The number of possible actions is finite. The agent will always need to choose from among a fixed number of possible actions as it was proved by results of the regression analysis in chapter 10. The change of parameters K_{trn} and K_{rot} does not have an effect on the emotional feedback of the human operator. Therefore, only four parameters (M_{trn}, D_{trn}, M_{rot}, D_{rot}) were selected as adjustable variables. We define a set of possible actions in the following way: the agent could apply two actions (increase or decrease) per each parameter and additional action "does nothing" when no change is required. The change of inertial and dumping components of the impedance controller leads to the change in the cart dynamics.

Figure 11.6: Set of actions

11.3 Rewards

In order to help the agent in the learning process we created a condition based reward structure. The most important part is the reward definition for the state. The agent goal is always the same - to maximize its total rewards. In our case we mostly use negative rewards (i.e. punishments) for the settings that could be recognized as bad. The reason for the negative rewards is the following. Due to the fact that the agent goal is to maximize cumulative rewards, if we used positive rewards the agent could get stuck in switching between the first states and would accumulate a very large cumulative reward even if the comfortable impedance controller settings were not found. In case of negative rewards the agent tried to minimize the punishment by searching the most convenient set of impedance controller settings. The result will be the set of impedance controller settings convenient for the current operator.

The reward system works as follows. The agent checks if the interaction dynamics is positive by comparing values of mean values and standard deviation for the current step and the previous step. Additionally, the agent checks if there is no emergency situation by analyzing the E-stop button state. Peaks of the interaction force have to be avoided as well. If a human operator thinks that the current settings are convenient for him he might give a positive feedback. In the end we sum up the rewards for different criteria. If none of the criteria were met the reward is set to the negative one.

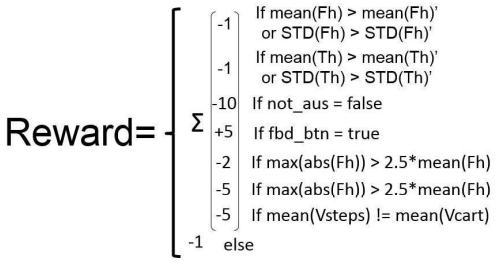

Figure 11.7: Rewards

11.4 High-level control

The learning algorithm that is used in the context of this thesis is called Q-Learning, which is a model-free Temporal-Difference (TD) algorithm. TD learning methods

combine the ideas behind Monte Carlo and dynamic programming methods. Therefore, a Q-Learning algorithm does not need a model just like Monte Carlo methods. Furthermore, TD methods update the state value directly after each step like dynamic programming methods.

$$\underbrace{TD(s_t, a_t)}_{\text{temporal difference}} = \underbrace{r(s_t, a_t)}_{\text{reward}} + \underbrace{\gamma}_{\text{discount factor}} \cdot \underbrace{\max_a Q(s_{t+1}, a_{t+1})}_{\text{estimate of optimal future value}} - \underbrace{Q(s_t, a_t)}_{\text{old value}}] \quad (11.1)$$

The discount factor is settled between 0 and 1. The purpose of the γ is to provide the mechanism for discounting of the future rewards. In other words, it allows us to choose a better option, because the value of receiving of a particular reward in the future is generally less than receiving the same reward now.

Another important equation is the Bellman's equation 11.2. The Bellman equation demonstrates what Q-value has to be used as the value for the action that was taken in the previous step. The equation includes a learning rate parameter α that defines how quickly Q-values are adjusted. Learning rate can take any value from 0 to 1.

$$\underbrace{Q_{new}(s_t, a_t)}_{\text{new value}} = \underbrace{Q_{old}(s_t, a_t)}_{\text{old value}} + \underbrace{\alpha}_{\text{learning rate}} \cdot \underbrace{TD(s_t, a_t)}_{\text{temporal difference}} \quad (11.2)$$

Q-Learning does only work with MDP's, because all values are calculated based on the current state. Therefore, each state instance must represent the entire configuration of the agent and environment. The basic Q-Learning update is defined by:

$$\underbrace{Q(s_t, a_t)}_{\text{new value}} \leftarrow \underbrace{Q(s_t, a_t)}_{\text{old value}} + \underbrace{\alpha}_{\text{learning rate}} \cdot [\underbrace{r(s_t, a_t)}_{\text{reward}} + \underbrace{\gamma}_{\text{discount factor}} \cdot \underbrace{\max_a Q(s_{t+1}, a_{t+1})}_{\text{estimate of optimal future value}} - \underbrace{Q(s_t, a_t)}_{\text{old value}}] \quad (11.3)$$

where $Q(s_t, a_t)$ represents the value for a cell in Q-matrix that demonstrates the choice of action a, form a state s at current time t. $r(s_t, a_t)$ is the reward received for the choice of action a, form state s.

The diagram shown in the figure 11.8 presents the process of Q-Learning. The process begins by initializing the Q-Table. This table represents the agent's policy on how to behave in the environment. In the next step the action for the current step has to be selected. There are two available options. One option is to choose the action with the highest Q-Value. Another option is to take a random action in order to explore the environment. The common strategy for resolution of the trade-off between exploration and exploitation is Epsilon-Greedy algorithm.

For each step within an episode, we set our exploration rate threshold to a random number between 0 and 1. This will be used to determine whether our agent will explore or exploit the environment in this time-step.

If the threshold is greater than the exploration rate, which is initially set to 1, then the agent will exploit the environment and choose the action that has the

highest Q-value in the Q-table for the current state. If, on the other hand, the threshold is less than or equal to the exploration rate, then the agent will explore the environment, and sample an action randomly.

As soon as the action is selected, the agent performs the action. When the action is performed the agent receives a reward. Based on the received reward and the information about the current state the TD is updated. Than the Q-Value for the current state was updated using the information about the current state, TD value and the Bellman's equation 11.2 and the agent switches to the next step.

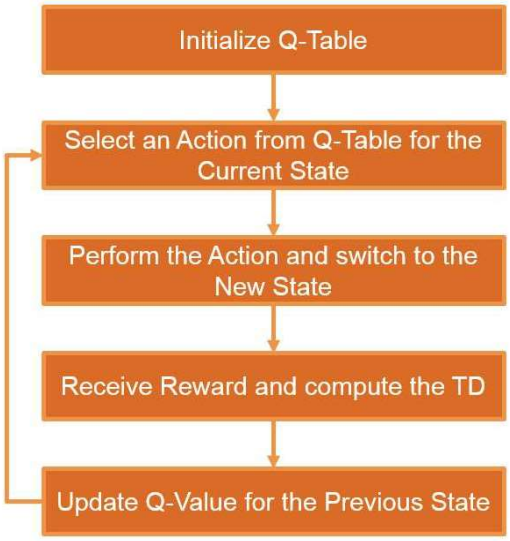

Figure 11.8: Q-learning process diagram

The diagram of the Q-Learning process could be presented in the shape of pseudo-code shown in the table 11.1.

The Q-Learning algorithm was implemented inside the high-level controller which is Raspberry Pi 4 in our case. Python language was used for implementation. The information about process values (interaction forces, odometry) is supplied to high-level controller from low-level controller using the serial port. Using the same link information about the actual impedance controller parameters provided to low-level controller. Protocol uses a CRC data check. The data of biological markers is read from a smart band using a BLE protocol. Console output of the learning process is shown in the figure 11.9. Information consists of the current episode number, the number of the step inside the episode, selected action, obtained reward and the new set of impedance controller parameters to be tested.

In the figure 11.10 you could find the graphic visualization of the Q-table values during the learning process. The yellow color represents the areas with the high rating and the blue color represents the areas with low rating. When we start the interaction process the values in Q-Table are equal to one another. However, as soon as the algorithm takes action the system state will be changed and corresponding value in Q-table will be updated according to the reward information. Quality and

Q-learning: Learn function $Q : \mathcal{X} \times \mathcal{A} \to \mathbb{R}$

Require:

Sates $\mathcal{X} = \{1, \ldots, n_x\}$

Actions $\mathcal{A} = \{1, \ldots, n_a\}$, $A : \mathcal{X} \Rightarrow \mathcal{A}$

Reward function $R : \mathcal{X} \times \mathcal{A} \to \mathbb{R}$

Black-box (probabilistic) transition function $T : \mathcal{X} \times \mathcal{A} \to \mathcal{X}$

Learning rate $\alpha \in [0, 1]$, typically $\alpha = 0.1$

Discounting factor $\gamma \in [0, 1]$

procedure QLEARNING($\mathcal{X}$, A, R, T, α, γ)

Initialize $Q : \mathcal{X} \times \mathcal{A} \to \mathbb{R}$ arbitrarily

while Q is not converged **do**

Start in state $s \in \mathcal{X}$

while s is not terminal **do**

Calculate π according to Q and exploration strategy (e.g. $\pi(x) \leftarrow \arg\max_a Q(x, a)$)

$a \leftarrow \pi(s)$

$r \leftarrow R(s, a)$ ▷ Receive the reward

$s' \leftarrow T(s, a)$ ▷ Receive the new state

$Q(s', a) \leftarrow (1 - \alpha) \cdot Q(s, a) + \alpha \cdot (r + \gamma \cdot \max_{a'} Q(s', a'))$

$s \leftarrow s'$

return Q

Table 11.1: Learn function of the Q-Learning algorithm presented in pseudo-code

speed of reinforcement learning process partially depends on the teacher. If human operator uses a user button to give a positive feedback or e-stop to give a negative feedback, it could significantly speed up the learning process.

When we have a look at Q-Learning dynamics by observing Q-Table changes in time the following information could be extracted. Q-Table is visualized by means of color map (heat map). From the first figure it is shown that in the first moments of the learning process the Q-Values are quite similar to each other. Significant area of the color map is colored in yellow. However, with time the color map gets more dark spots by receiving the negative feedback about the impedance controller settings. In the long run it is depicted that the major area of the color map is covered by dark blue and green colors that demonstrates negative effect of the impedance controller setting on the interaction process. Only tiny yellow line is presented in the color map. This line represents the impedance controller settings that fully respond to the human-operator intention. It is possible to obtain the impedance controller settings by selecting the state that corresponds to maximum value of the Q-Table.

```
Episode 36
Step 189
Current action Mdown
State_num 0
New state [2, 20, 1, 10]
Reward -1
Episode 36
Step 190
Current action Jup
State_num 4
New state [2, 20, 4, 10]
Reward -1
Episode 36
Step 191
Current action Drup
State_num 5
New state [2, 20, 4, 20]
Reward -1
Episode 36
Step 192
Current action Dtdown
State_num 0
New state [2, 20, 1, 10]
Reward -1
Episode 36
```

Figure 11.9: Console output of the learning process

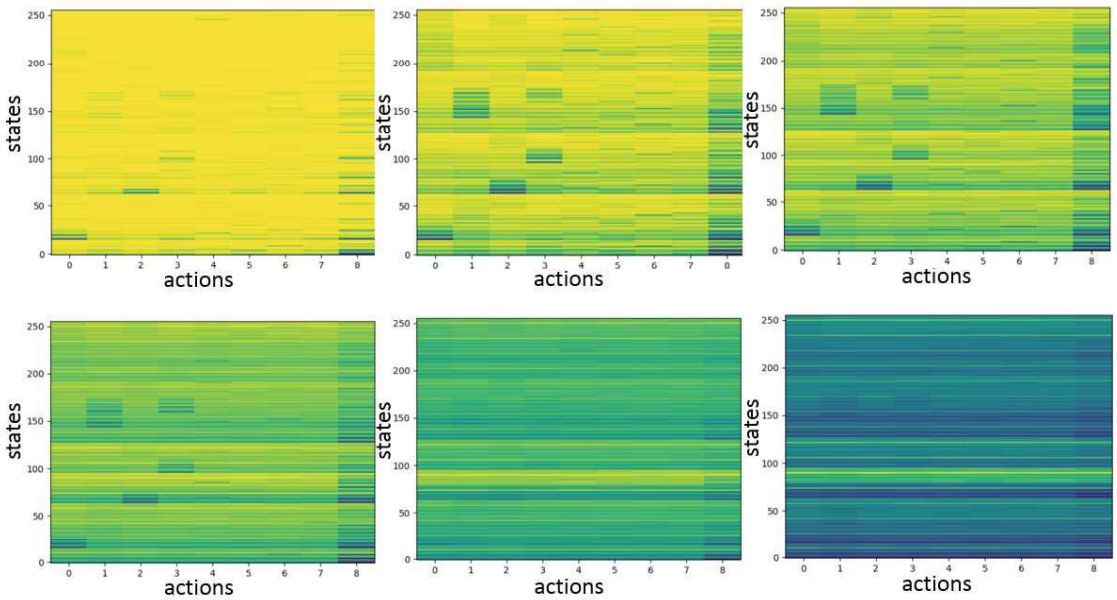

Figure 11.10: Dynamic change of the Q-value during the learning process

12 Conclusion

> "Perfection is achieved, not when there is nothing more to add, but when there is nothing left to take away."
>
> Antoine de Saint Exupery

In the course of this work we have systematized the existing theory in the field of pHRI related to human in-the-loop study while interacting with powered mobile platform. A mathematical and experimental model of the industrial power assisted cart was developed. A great amount of work was performed in powered mobile platform programming and control system implementation.

The work brings significant contribution to the area of pHRI by developed workflow that includes experimental platform development, experiment design and evaluation of the results using regression analysis and development of adaptive impedance controller that is suitable to perform collaborative tasks. Personality-oriented scheme presented in this work results in efficient physical interaction that responds to the intentions of the human-operator as well as it enhances the user comfort during the process of a carrying task.

This work also brings contribution to the area of raw data analysis and feature detection. We tested interaction with different loads and on different types of trajectories such as 5 meters strait drive, round and 8-like shape trajectory, a complex predefined path and a free ride. All the experiments were performed in the indoor environment.

The control system with the impedance controllers of rotational and translational motion was implemented in the experimental platform. It allows to support human operator during linear dive and turns. It helped to obtain the dynamics relevant to the material handling task. Analysis of interaction characteristics allowed us to identify the physical measures, emotional feedback as well as biological markers which were used as additional sources of information to improve interaction.

We evaluated the effects of the controller' settings of the operator's comfort and developed a system of automatic tuning of parameters. One of AI methods was applied to the developed powered industrial cart. The method called Q-learning belongs to the area of reinforcement learning. It allows the powered cart to learn the desired intention of the human-operator by means of rewards for different settings of impedance controllers. In the end it was possible to find out the set of

settings that refers to the highest comfort level and sufficient performance for a particular operator. The RL algorithm was implemented in the microcomputer Raspberry Pi using Python language. This controller was called a high-level controller. The low-level control was implemented in the microprocessor ATmega2560 (Arduino board). It includes mathematical description of cart dynamics and kinematics as well as impedance controllers for translational and rotational motion of the cart and PID controller for the powered wheels.

In addition, the applications for BLDC drive control, load cell control and configuration software, C-Sharp based hardware extension library for Rasberry Pi and Matlab were developed. It allows to run real-time target based simulation using math apparatus of Matlab in combination with low-cost embedded sensors and drives. More information could be found in appendix to this work.

Accumulated results suggest promising ideas for the future work. In particular, the number of involved experienced and inexperienced human operators (males and females) could be increased. It allows to contribute into discovered correlation (dependency) between operator's comfort and impedance controller's settings. Furthermore, a combination of the results with industrial pHRI scenarios, where human comfort is set as a significant measure, allows to optimize operator's tasks and logistic processes in plant simulation. Optimized tasks and processes could be applied at the real factory that brings significant value to the end customer in the form of drastic reduction of sick leave requests caused by transportation hazards.

In the end of the work I would like to express my gratitude to the people who supported me during the research and showed me the importance of my research. I am glad that my research made a contribution to the future development of human-robot co-existence and cooperation.

13 Internship

I did my internship in Linz Center of Mechatronics GmbH at the Department of Sensors & Communication. This company is located in the Since Park of Johannes-Kepler University, Austria. The LCM team has comprehensive experience in tendering for EU projects and other international project plans. Project proposals for the following national programmes and structural funds were submitted: ETP: European Technology Platforms: Initiative to support international networking. Funding: Horizon 2020 – Rules for Participation (100/70%) | JTIs: JTI – Joint Technology Initiatives: public-private partnership to support transnational research collaboration in selected technological fields | cPPPs: contractual Public Private Partnerships | EIPs: European Innovation Partnerships | ERANET: European Research Area | EIT (KICs): European Innovation and Technology Institute – Knowledge and Innovation Communities | HORIZON2020: research programm from the eu commission | FET: Future and Emerging Technologies | Art. 185-Initiativen. Some of the results of these projects have since been successfully brought onto the market.

Figure 13.1: Linz Center of Mechatronics GmbH

As an intern I participated in several research and commercial projects related to the indoor navigation applications and human motion detection. Working with outstanding professionals I developed a cross-platform application that allowed to add a network interface to any USB (UART) device (USB - Universal Serial Bus). Writ-

ing documentation including API (Application Programming Interface) description and created an application sample was significant part of the work.

I was happy to help modify and optimize UART(Universal Asynchronous Receiver-Transmitter) data transfer protocol in order to use DMA (Direct Memory Access).

In the framework of another project, I was designing and implementing the software for MEMS (Microelectromechanical systems) sensors reading. In addition, I was among the developers to create software for MEMS data visualization. At a later stage of the project we improved and extended the MEMS sensor library.

Implementing the algorithm for human motion detection was a project that helped me to learn a lot. I transmitted features activation information to a base station. Last but not least, I was able to design and implement a wireless network sniffer for debugging of indoor positioning systems (IPS) shown in the figure 13.

It was a priceless experience as it helped me to raise my knowledge and skills to a new level. I acquired competences in the areas of indoor navigation and digital signal processing in the field of human motion detection. The internship deepened my knowledge of python multi tasking and C++ in the field of embedded systems.

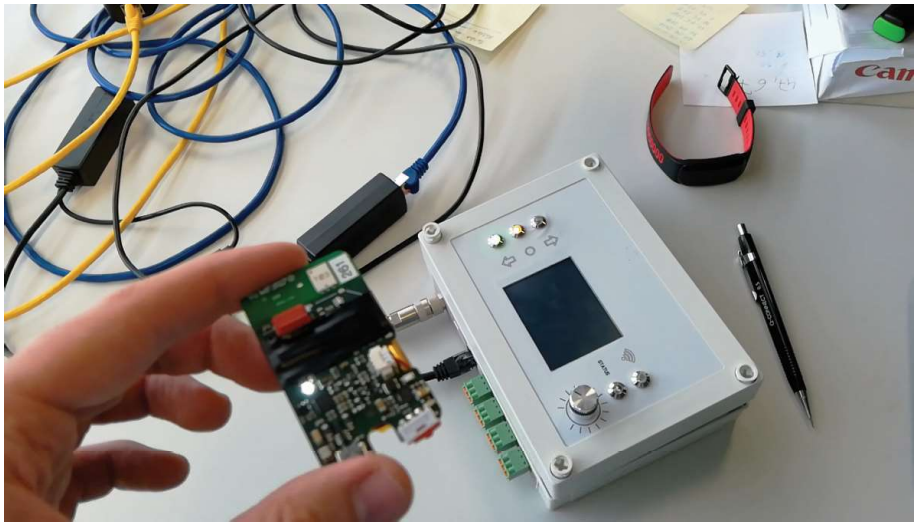

Figure 13.2: Developed indoor positioning system

14 Publications

1. KOCHUBEY, Dmitry; TUMA, Petr. Industrial Cart Power Assistance on Undefined Path. In: Proceedings of the 11th PErvasive Technologies Related to Assistive Environments Conference. Corfu, Greece: Association for Computing Machinery, 2018, pp. 108–109. PETRA '18. ISBN 9781450363907. Available from DOI: 10.1145/3197768.3203174.

2. KOCHUBEY, Dmitry; TUMA, Petr. Human Comfort and Skill Evaluation During Interaction with PAMV. In: Proceedings of the 10th International Conference on PErvasive Technologies Related to Assistive Environments. Island of Rhodes, Greece: Association for Computing Machinery, 2017, pp. 250–251. PETRA '17. ISBN 9781450352277. Available from DOI: 10.1145/3056540. 3076213.

15 Appendix

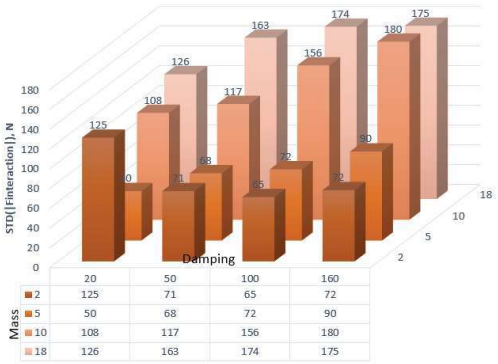

Figure 15.1: Standard deviation of absolute interaction force for different settings of impedance controller. Sample 1.

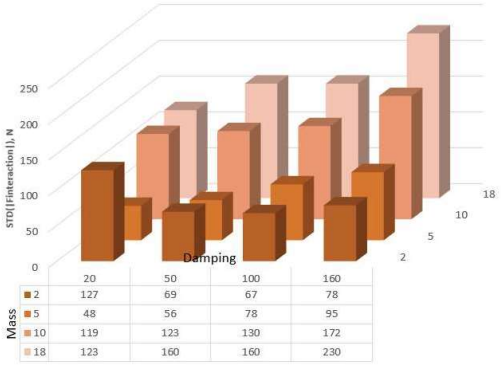

Figure 15.2: Standard deviation of absolute interaction force for different settings of impedance controller. Sample 2.

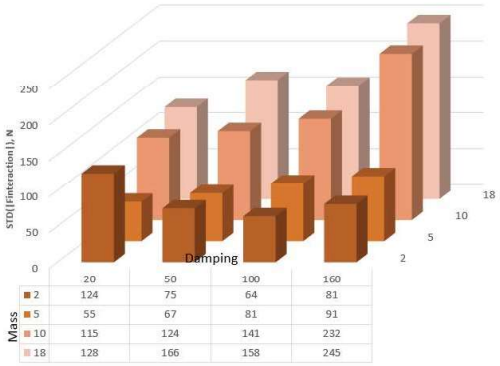

Figure 15.3: Standard deviation of absolute interaction force for different settings of impedance controller. Sample 3.

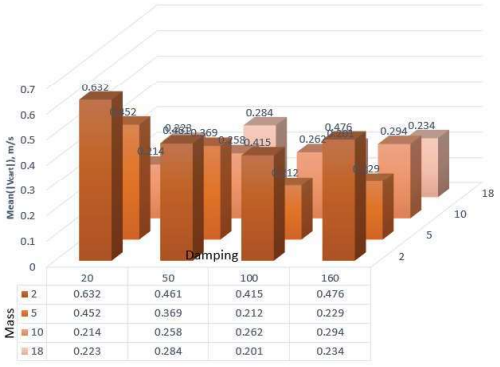

Figure 15.4: Mean value of absolute cart velocity for different settings of impedance controller. Sample 1.

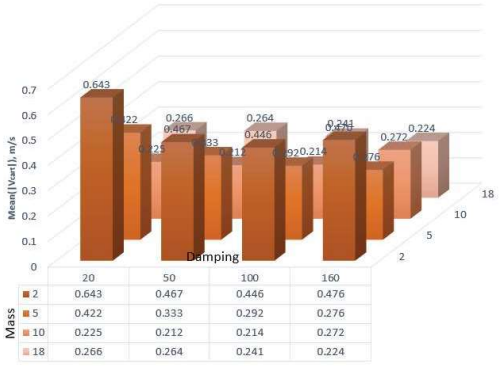

Figure 15.5: Mean value of absolute cart velocity for different settings of impedance controller. Sample 2.

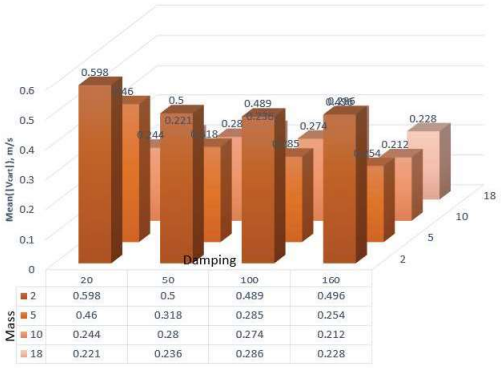

Mass \ Damping	20	50	100	160
2	0.598	0.5	0.489	0.496
5	0.46	0.318	0.285	0.254
10	0.244	0.28	0.274	0.212
18	0.221	0.236	0.286	0.228

Figure 15.6: Mean value of absolute cart velocity for different settings of impedance controller. Sample 3.

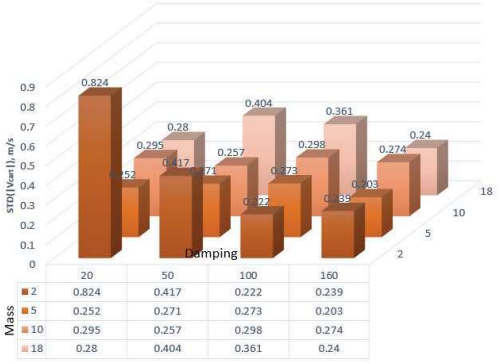

Mass \ Damping	20	50	100	160
2	0.824	0.417	0.222	0.239
5	0.252	0.271	0.273	0.203
10	0.295	0.257	0.298	0.274
18	0.28	0.404	0.361	0.24

Figure 15.7: Mean value of absolute cart velocity for different settings of impedance controller. Sample 1.

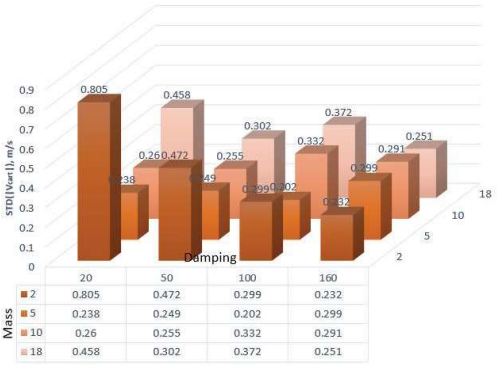

Mass \ Damping	20	50	100	160
2	0.805	0.472	0.299	0.232
5	0.238	0.249	0.202	0.299
10	0.26	0.255	0.332	0.291
18	0.458	0.302	0.372	0.251

Figure 15.8: Mean value of absolute cart velocity for different settings of impedance controller. Sample 2.

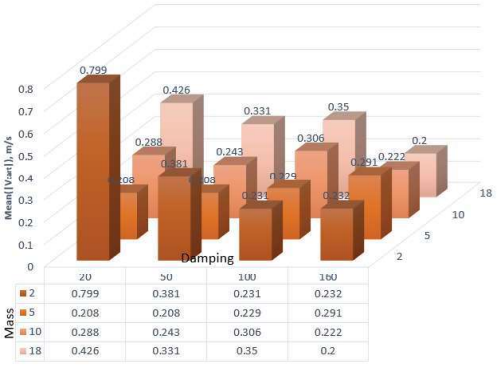

Figure 15.9: Mean value of absolute cart velocity for different settings of impedance controller. Sample 3.

Bibliography

[1] BANERJEE, S.; CHATTOPADHYAY, D.P. Studies on energy expenditure of rickshaw pullers. *Indian Journal of Physiology and Pharmacology*. 1959, no. 3, pp. 147–160.

[2] HAISMAN, M.F.; WINSMANN, F.R.; GOLDMAN, R.F. Energy cost of pushing loaded handcarts. *Journal of Applied Physiology*. 1972, no. 33, pp. 181–183.

[3] JÄGER, M.; LUTTMANN, A.; LAURIG, W. The load on the spine during the transport of dustbins. *Applied Ergonomics*. 1984, no. 15, pp. 91–98.

[4] SCHIBYE, B.; SØGAARD, K.; MARTINSEN, D.; KLAUSEN, K. Mechanical load on the low back and shoulders during pushing and pulling of two-wheeled waste containers compared with lifting and carrying of bags and bins. *Clinical Biomechanics*. 2001, no. 16, pp. 549–559.

[5] ERGOWEB, Darcor in cooperation with. The ergonomics of manual material handling. Pushing and pulling tasks. *Darcor*. 2014, no. 37(4), pp. 1–28.

[6] HOOZEMANS, Marco; BEEK, Allard van der; FRINGS-DRESEN, Monique; WOUDE, Lucas; DIJK, Frank. Low-back and shoulder complaints among workers with pushing and pulling tasks. *Scandinavian journal of work, environment health*. 2002, vol. 28, pp. 293–303. Available from DOI: 10.5271/sjweh.678.

[7] HARKNESS, Elaine; MACFARLANE, Gary; NAHIT, Elizabeth; SILMAN, A.J.; MCBETH, J. Mechanical and psychosocial factors predict new onset shoulder pain: A prospective cohort study of newly employed workers. *Occupational and environmental medicine*. 2003, vol. 60, pp. 850–7.

[8] ABEL, E.; FRANK, T. The design of attendant propelled wheelchairs. *Prosthetics and Orthotics International*. 1991, vol. 15, pp. 38–45.

[9] GARG, Arun; WATERS, Thomas R.; KAPELLUSCH, Jay M.; KARWOWSKI, Waldemar. Psychophysical basis for maximum pushing and pulling forces: A review and recommendations. *International journal of industrial ergonomics*. 2014, vol. 44 2, pp. 281–291.

[10] SNOOK, George A. The father of sports medicine. *The American Journal of Sports Medicine*. 1978, vol. 6, no. 3, pp. 128–131. Available from DOI: 10.1177/036354657800600306. PMID: 350061.

[11] FRYMOYER, JW; POPE, MH; COSTANZA, MC; ROSEN, JC; GOGGIN, JE; WILDER, DG. Epidemiologic studies of low-back pain. *Spine*. 1980, vol. 5, no. 5, pp. 419–423. ISSN 0362-2436. Available from DOI: 10.1097/00007632-198009000-00005.

[12] CHAFFIN, DON B. Manual Materials Handling and the Biomechanical Basis for Prevention of Low-Back Pain in Industry—An Overview. *American Industrial Hygiene Association Journal*. 1987, vol. 48, no. 12, pp. 989–996. Available from DOI: 10.1080/15298668791385967. PMID: 2963515.

[13] *Statistics A-Z*. 2017. Available also from: http://ec.europa.eu/eurostat/data/statistics-a-z/abc/.

[14] KUMAR, S.; NARAYAN, Y.; BACCHUS, C. Symmetric and asymmetric two-handed. *Hum Factors*. 1995, no. 37 (4), pp. 854–865.

[15] DIN, ENISO. *10218–2.: Robots and Robotic Devices–Safety Requirements For Industrial Robots–Part 2: Robot Systems and Integration*. Beuth Verlag GmbH, Berlin, 2012.

[16] SNOOK, Stover H.; CIRIELLO, Vincent M. The design of manual handling tasks: revised tables of maximum acceptable weights and forces. *Ergonomics*. 1991, vol. 34, no. 9, pp. 1197–1213. Available from DOI: 10.1080/00140139108964855. PMID: 1743178.

[17] CIRIELLO, V. M.; SNOOK, S. H.; HASHEMI, L.; COTNAM, J. Distributions of manual materials handling task. *International Journal of Industrial Ergonomics*. 1999, no. 24, pp. 379–388.

[18] CIRIELLO, V.M.; MCGORRY, R.W.; MARTIN, S.E. Maximum acceptable horizontal and vertical forces of dynamic pushing on high and low coefficient of friction floors. *International Journal of Industrial Ergonomics*. 2001, no. 27, pp. 1–8.

[19] NAGAMI, A.; MURAKAMI, T.; OHNISHI, K. *Industrial Electronics Society, 2003. IECON '03. The 29th Annual Conference of the IEEE*. A Power-Assistant Platform Taking Environmental Disturbance into Account. 2000.

[20] HOGAN, N. Impedance Control: an Approach to Manipulation: Part I-III. *SME Journal of Dynamic Systems, Measurement, and Control*. 1985, vol. 107, pp. 1–24.

[21] ALMEIDA, F.; A.LOPES; ABREU, P. *Force-Impedance Control: a new control strategy of robotic manipulators*. 1999.

[22] SHARIFI, M.; BEHZADIPOUR, S.; VOSSOUGHI, G. Nonlinear model reference adaptive impedance control for human–robot interactions. *Control Engineering Practice*. 2014, no. 32, pp. 9–27.

[23] MIYAZAWA, T.; KATSURA, S.; OHNISHI, K. *A Power-Assisted Wheelchair Taking Running Environment into Account*. 2003. No. 2.

[24] DUCHAINE, V.; GOSSELI, C. General Model of Human-Robot Cooperation Using a Novel Velocity Based Variable Impedance Control. *IEEE/WHC*. 2007, pp. 1–24.

[25] TERASHIMA, K.; WATANABE, K.; UENO, Y.; MASUI, Y. Auto-Tuning Control of Power Assist System Based on The Estimation of Operator's Skill Level for Forward and Backward Driving of Omni-Directional Wheelchair. *IEEE/RSJ International Conference on Intelligent Robots and Systems (IROS)*. 2010, no. 37(4), pp. 6046–6051.

[26] SILVA, L. A.; RODRIGUES, L.A.; CARDOSO, B.J. Methodology for rating three phase induction motors to drive vehicles used by collectors of recyclable materials. *Brazilian Symposium on Intelligent Automation*. 2011, no. 3, pp. 1346–1351.

[27] SILVA, L. A.; JUSTINO, J.; CARDOSO, B.J.; PUJATTI, F. Design and Implementation of a Low-Cost Robotic Load Carrier. *IEEE International Conference on Robotics and Automation*. 2014, no. 3, pp. 2731–2737.

[28] KOCHUBEY, Dmitry; TUMA, Petr. Human Comfort and Skill Evaluation During Interaction with PAMV. In: *Proceedings of the 10th International Conference on PErvasive Technologies Related to Assistive Environments*. Island of Rhodes, Greece: Association for Computing Machinery, 2017, pp. 250–251. PETRA '17. ISBN 9781450352277. Available from DOI: 10.1145/3056540.3076213.

[29] *HX711 24-Bit Analog-to-Digital Converter (ADC) for Weigh Scales*. 2014. No. HX711. Rev. 1.0.

[30] *AS5045 12-Bit Programmable Magnetic Rotary Position Sensor*. 2017. No. AS5045. v2-01.

[31] *HMC5983 3-Axis Digital Compass IC*. 2012. No. HMC5983. 900425.

[32] *MPU-6000/MPU-6050 Register Map and Descriptions*. 2013. No. MPU6050. Revision 4.2.

[33] SAUNDERS, J.; INMAN, Verne; EBERHART, Howard. Major determinants in normal and pathological gait. *The Journal of bone and joint surgery. American volume*. 1953, vol. 35-A, pp. 543–58. Available from DOI: 10.2106/00004623-195335030-00003.

[34] KUO, Arthur D.; DONELAN, J. Maxwell. Dynamic Principles of Gait and Their Clinical Implications. *Physical Therapy*. 2010, vol. 90, no. 2, pp. 157–174. ISSN 0031-9023. Available from DOI: 10.2522/ptj.20090125.

[35] MARTINI, F.; TIMMONS, M.J.; TALLITSCH, R.B. *Human Anatomy*. Pearson Benjamin Cummings, 2012. ISBN 9780321688156. Available also from: https://books.google.cz/books?id=loaWbwAACAAJ.

[36] BURDET, E.; FRANKLIN, D. W.; OSU, R.; TEE, K. P.; KAWATO, M.; MILNER, T. E. How are internal models of unstable tasks formed? In: *The 26th Annual International Conference of the IEEE Engineering in Medicine and Biology Society*. 2004, vol. 2, pp. 4491–4494.

[37] CHOUDHURY, T. T.; RAHMAN, M. M.; KHORSHIDTALAB, A.; KHAN, M. R. Modeling of Human Arm Movement: A Study on Daily Movement. In: *2013 Fifth International Conference on Computational Intelligence, Modelling and Simulation*. 2013, pp. 63–68.

[38] ARTEMIADIS, P. K.; KATSIARIS, P. T.; LIAROKAPIS, M. V.; KYRIAKOPOULOS, K. J. Human arm impedance: Characterization and modeling in 3D space. In: *2010 IEEE/RSJ International Conference on Intelligent Robots and Systems*. 2010, pp. 3103–3108.

[39] TEE, K P; BURDET, E; CHEW, C M; MILNER, T E. A model of force and impedance in human arm movements. *Biological cybernetics*. 2004, vol. 90, pp. 368–375.

[40] SPEICH, John; SHAO, Liang; GOLDFARB, Michael. Modeling the human hand as it interacts with a telemanipulation system. *Mechatronics*. 2005, vol. 15, pp. 1127–1142. Available from DOI: 10.1016/j.mechatronics.2005.06.001.

[41] RAHMAN, M. M.; IKEURA, R.; MIZUTANI, K. Investigating the impedance characteristic of human arm for development of robots to co-operate with human operators. In: *IEEE SMC'99 Conference Proceedings. 1999 IEEE International Conference on Systems, Man, and Cybernetics (Cat. No.99CH37028)*. 1999, vol. 2, 676–681 vol.2.

[42] WANG, S; ZUO, G; XU, J; ZHENG, H. *Biomedical Engineering and Informatics (BMEI), 2011 4th International Conference*. IEEE, 2011.

[43] TANAKA, Y.; KASHIBA, Y.; YAMADA, N.; SUETOMI, T.; NISHIKAWA, K.; NOUZAWA, T.; TSUJI, T. Active-steering control system based on human hand impedance properties. In: *2010 IEEE International Conference on Systems, Man and Cybernetics*. 2010, pp. 1697–1702.

[44] LEE, K.S.; CHAFFIN, D.B.; HERRIN, G.D.; WAIKAR, A.M. Effect of handle height on lower-back. *Applied Ergonomic*. 1991, no. 2(2), pp. 117–123.

[45] COMPANY, T.E.K. *Kodak's Ergonomic Design for People at Work*. Wiley, 2003. ISBN 9780471418634. Available also from: https://books.google.cz/books?id=l39RAAAAMAAJ.

[46] BORG, Gunnar A.V. Psychophysical bases of percived exertion. *Medicine and science in sports and exercise*. 1982, no. 14(5), pp. 377–381.

[47] ALIAN, Aymen; SHELLEY, Kirk. Photoplethysmography: Analysis of the Pulse Oximeter Waveform. 2014, pp. 165–178. ISBN 978-1-4614-8556-8. Available from DOI: 10.1007/978-1-4614-8557-5_19.

[48] AGUILAR PELAEZ, Eduardo; VILLEGAS, Esther. LED power reduction trade-offs for ambulatory pulse oximetry. *Conference proceedings : ... Annual International Conference of the IEEE Engineering in Medicine and Biology Society. IEEE Engineering in Medicine and Biology Society. Conference*. 2007, vol. 2007, pp. 2296–9. Available from DOI: 10.1109/IEMBS.2007.4352784.

[49] REISNER, Andrew; SHALTIS, Phillip; MCCOMBIE, Devin; ASADA, Harry. Reisner A, Shaltis PA, McCombie D, Asada HH. Utility of the photoplethysmogram in circulatory monitoring. *Anesthesiology*. 2008, vol. 108, pp. 950–8. Available from DOI: 10.1097/ALN.0b013e31816c89e1.

[50] *MC3413 3-Axis Accelerometer Preliminary Datasheet*. 2014. No. MC3413. Revision 1.7.

[51] KOCHUBEY, Dmitry; TUMA, Petr. Industrial Cart Power Assistance on Undefined Path. In: *Proceedings of the 11th PErvasive Technologies Related to Assistive Environments Conference*. Corfu, Greece: Association for Computing Machinery, 2018, pp. 108–109. PETRA '18. ISBN 9781450363907. Available from DOI: 10.1145/3197768.3203174.

[52] STULP, F.; BUCHLI, J.; ELLMER, A.; MISTRY, M.; THEODOROU, E.; SCHAAL, S. Reinforcement learning of impedance control in stochastic force fields. In: *2011 IEEE International Conference on Development and Learning (ICDL)*. 2011, vol. 2, pp. 1–6.

[53] *Decision Processes*. 2018. Available also from: https://artint.info/html/ArtInt_224.html.

[54] SUTTON, R.S.; BARTO, A.G. *Reinforcement Learning: An Introduction*. MIT Press, 2018. Adaptive Computation and Machine Learning series. ISBN 9780262039246. Available also from: https://books.google.cz/books?id=6DKPtQEACAAJ.

[55] SWAMYNATHAN, Manohar. Step 6 – Deep and Reinforcement Learning. In: *Mastering Machine Learning with Python in Six Steps: A Practical Implementation Guide to Predictive Data Analytics Using Python*. Berkeley, CA: Apress, 2017, pp. 297–344. ISBN 978-1-4842-2866-1. Available from DOI: 10.1007/978-1-4842-2866-1_6.

[56] WATKINS, Christopher. Learning From Delayed Rewards. 1989.